ELSEVIER

Contents lists available at ScienceDirect

# Food and Chemical Toxicology

journal homepage: www.elsevier.com/locate/foodchemtox





# Resolving complexity: Identification of altersetin and toxin mixtures responsible for the immunomodulatory, antiestrogenic and genotoxic potential of a complex *Alternaria* mycotoxin extract

Vanessa Partsch<sup>a,b</sup>, Francesco Crudo<sup>a,\*</sup>, Daniel Piller<sup>a</sup>, Elisabeth Varga<sup>a,c</sup>, Giorgia Del Favero<sup>a,d</sup>, Doris Marko<sup>a</sup>

- <sup>a</sup> University of Vienna, Faculty of Chemistry, Department of Food Chemistry and Toxicology, 1090, Vienna, Austria
- <sup>b</sup> University of Vienna, Faculty of Chemistry, Doctoral School in Chemistry, 1090, Vienna, Austria
- <sup>c</sup> University of Veterinary Medicine Vienna, Clinical Department for Farm Animals and Food System Science, Centre for Food Science and Veterinary Public Health, Unit Food Hygiene and Technology, 1210, Vienna, Austria
- <sup>d</sup> University of Vienna, Faculty of Chemistry, Core Facility Multimodal Imaging, 1090, Vienna, Austria

#### ARTICLE INFO

Handling Editor: Dr. Bryan Delaney

Keywords: Alternatia alternatia Food contaminants Toxicity-guided fractionation Combinatory effects In vitro toxicity

#### ABSTRACT

Alternaria mycotoxins may pose significant risks to human health due to their diverse spectrum of adverse effects and frequent occurrences in food. A previous study demonstrated the immunosuppressive, antiestrogenic, and genotoxic potential of a complex Alternaria mycotoxin extract (CE). The present study aimed to elucidate specific Alternaria mycotoxins or combinations thereof responsible for toxicity.

Following toxicity-guided fractionation of the CE, a multiparametric panel of assays was applied to assess different endpoints. These included immunomodulatory effects (NF- $\kappa$ B reporter gene assay in THP1-Lucia<sup>TM</sup> monocytes), estrogenicity/antiestrogenicity (alkaline phosphatase assay in Ishikawa cells) and genotoxicity ( $\gamma$ H2AX and alkaline comet assays in HepG2 cells).

LC-MS/MS analysis revealed prominent mycotoxins in the active fractions, with altersetin (AST) identified as a novel key compound exhibiting immunoinhibitory ( $\geq 2~\mu M$ ) and antiestrogenic ( $\geq 5~\mu M$ ) properties *in vitro*. Additionally, while specific mycotoxin combinations explained the toxicity of active fractions, some effects remained unexplained, suggesting the presence of unidentified bioactive substances.

This study underscores the significance of AST and specific toxin mixtures as major contributors to CE toxicity. Further, it highlights the importance of considering combinatory effects in risk assessment of *Alternaria* mycotoxins as well as further investigation of unknown *Alternaria* metabolites, which may pose additional health risks.

## Abbreviations

Altenuic acid III	AA-III			
Aryl hydrocarbon receptor	AhR			
Alkaline phosphatase	AlP			
Altenusin	ALS			
Altenuene	ALT			
Alterperylenol	ALTP			
Alternariol monomethyl ether	AME			
Alternariol	AOH			
AhR nuclear translocator	ARNT			
Altersetin	AST			
Altertoxin-I	ATX-I			
Altertoxin-II	ATX-II			
	(continued on next column)			

## (continued)

Boyine serum albumin	BSA
Charcoal-stripped FBS	CD-FBS
Complex Alternaria mycotoxin extract	CE
Cytochrome P450	CYP
4',6-diamidine-2'-phenylindoledihydrochloride	DAPI
Dexamethasone	Dexa
Dulbecco's Modified Eagle Medium/F12	DMEM/F12
Dimethyl sulfoxide	DMSO
Doxorubicin	Doxo
17β-estradiol	E2
Fetal bovine serum	FBS
Isoaltenuene	isoALT
Liquid chromatography tandem mass spectrometry	LC-MS/MS

(continued on next page)

<sup>\*</sup> Corresponding author. Department of Food Chemistry and Toxicology, University of Vienna, Währinger Str. 38, 1090, Vienna, Austria. E-mail address: francesco.crudo@univie.ac.at (F. Crudo).

#### (continued)

Lipopolysaccharide	LPS
Minimum Essential Medium	MEM
Penicillin streptomycin	P/S
Phosphate buffered saline	PBS
Pooled fractions of Alternaria extract	F
Reversed-phase high performance liquid chromatography	RP-HPLC
Single fractions of Alternaria extract	SF
Single mixtures	SM
Supercritical fluid chromatography	SFC
Standard deviation	SD
Stemphyltoxin III	STTX-III
Test over control	T/C
Tenuazonic acid	TeA
Tentoxin	TEN

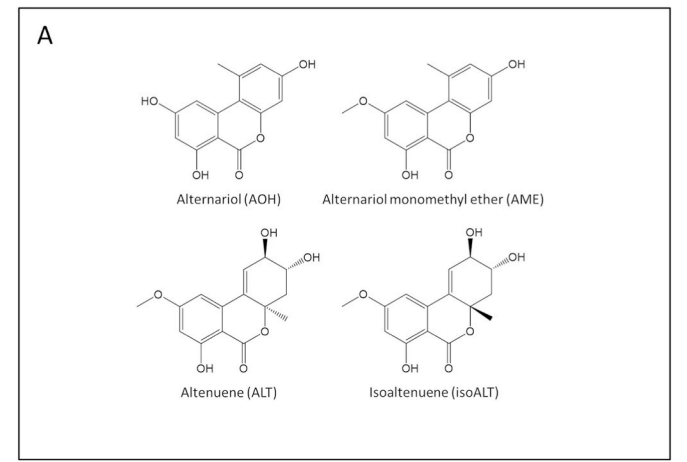
#### 1. Introduction

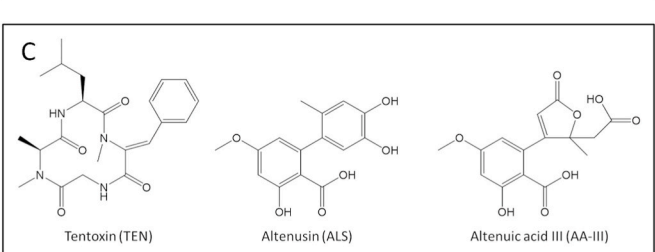
Fungi of the genus Alternaria can produce a broad spectrum of structurally different secondary toxic metabolites known as Alternaria mycotoxins. Unlike other mycotoxins, such as aflatoxins and fumonisins produced by Aspergillus and Fusarium strains respectively, which are regulated by the Commission Regulation (EU) 2023/915/2006, Alternaria mycotoxins are still classified as 'emerging mycotoxins' (European Commission, 2023; Gruber-Dorninger et al., 2017). The filamentous Alternaria fungi grow ubiquitously and can infest various substrates while displaying tolerance to different environmental conditions, including temperature and moisture variations (Aichinger et al., 2021). Pertaining the toxins, they are commonly found in grains, tomatoes, and their respective products, as well as in sunflower seeds and oil, fruits, beer, and wine (EFSA, 2011). So far, more than 70 Alternaria toxins have been isolated and chemically characterized. Based on their chemical structures, they can be categorized into different groups. A selection of mycotoxins and the respective classification are depicted in Fig. 1 (Crudo et al., 2019; Hellwig et al., 2002; Ostry, 2008).

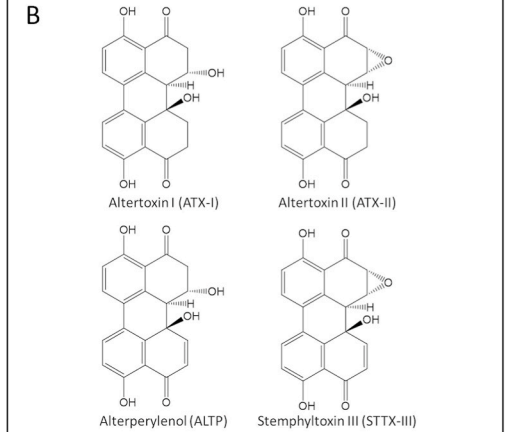
Some members of this class of mycotoxins are frequently detected in

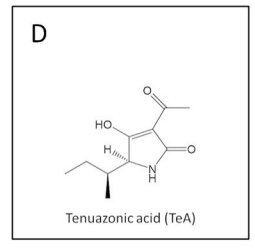
food at rather high concentrations and thus may endanger human health, especially that of the most exposed individuals such as vegetarians and toddlers (Arcella et al., 2016). Over the past decades, a wide range of adverse effects caused by some of the known Alternaria mycotoxins was identified. For example, both single mycotoxins and complex mixtures were shown, amongst others, to cause genotoxic, mutagenic, immunotoxic and estrogenic/antiestrogenic effects in vitro (Crudo et al., 2019; Louro et al., 2024). With regard to the immunomodulatory effects, the perylene quinone altertoxin II (ATX-II) and the dibenzo-α-pyrone AOH are known to suppress the lipopolysaccharide-induced inflammation and target the NF-kB signaling pathway in THP1 monocytes and macrophages (Crudo and Partsch et al., 2024; Del Favero et al., 2020; Kollarova et al., 2018). Among the Alternaria toxins exerting genotoxic effects, AOH and AME were reported to induce DNA strand breaks and act as topoisomerase poisons in various cell lines (Fehr et al., 2009; Pfeiffer et al., 2007). Moreover, both compounds were described to induce oxidative stress, which might contribute to their genotoxic potential (Aichinger et al., 2017; Tiessen et al., 2013). Upon toxicity-guided fractionation, the epoxide-bearing perylene quinone ATX-II was identified as a potent genotoxic compound, exceeding by far the effects caused by AOH and AME. Unlike the latter, this epoxide-carrying metabolite was postulated to form DNA adducts (Schwarz et al., 2012b).

So far, research has mainly focused on individual *Alternaria* mycotoxins, not taking into consideration the potential overlay of effects caused by the natural co-occurrence of multiple mycotoxins. Facing this issue, a study carried out by Aichinger et al. (2019) unexpectedly showed that a complex *Alternaria* mycotoxin extract (CE), obtained by cultivation of an *Alternaria alternata* strain on long rice, exerted antiestrogenic effects, despite the presence of the well-known mycoestrogens AOH and AME (Aichinger et al., 2019; Lehmann et al., 2006). Additionally, Crudo and Partsch et al. (2024) showed the ability of the CE to also to suppress effectively LPS-induced activation of the NF-κB signaling pathway. By toxicity-guided fractionation the perylene quinones ATX-I and ALTP were identified as novel contributors to the immunosuppressive and antiestrogenic properties of complex *Alternaria* 









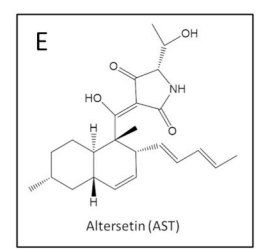


Fig. 1. Chemical structures of selected *Alternaria* mycotoxins. The compounds are categorized based on their chemical structures: A) dibenzo-α-pyrones, B) perylene quinones, C) *Alternaria* mycotoxins with miscellaneous structures, D) tetramic acid derivatives, E) others.

toxin mixtures. However, the contribution of these mycotoxins to the overall immunosuppressive and antiestrogenic effects of the CE was limited, arguing for the presence of other active contributors still to be identified.

Apart for its immunosuppressive and antiestrogenic effects, the CE was also found to exert genotoxic effects, although the potency of the extract exceeded the expected sum of the genotoxic constituents identified so far (Aichinger et al., 2019). To summarize, the currently available data point towards the presence of unknown or yet uninvestigated active Alternaria mycotoxins in the CE or the occurrence of combinatory effects between multiple mycotoxins. Taking all this into consideration, it appears more crucial than ever to also investigate combinations of different Alternaria mycotoxins, to complement the existing data of isolated single compounds. Therefore, in the present study a complex Alternaria alternata extract with known genotoxic, immunosuppressive and antiestrogenic properties was selected to identify the Alternaria mycotoxins and/or their combinations responsible for its various toxicological effects. A toxicity-guided fractionation approach by reversed-phase high performance liquid chromatography (RP-HPLC) was applied and the obtained fractions were examined from a chemical and toxicological point of view. In detail, the fractions were analyzed through a liquid chromatography-tandem mass spectrometry (LC-MS/MS) multi-method and investigated with respect to immunomodulatory, antiestrogenic and genotoxic potential. Based on the quantitative LC-MS/MS data, the most abundant mycotoxins in the active fractions were chosen to be examined singularly and in naturally occurring combinations.

#### 2. Materials and methods

#### 2.1. Materials

Acetonitrile and the 25 % ammonia solution were acquired from Honeywell International Inc. (Morristown, USA), while LC-MS grade methanol and ethanol were purchased from Thermo Fisher Scientific Inc. (Waltham, USA). Formic acid and LC-MC grade water were bought from VWR International (Pennsylvania, USA), and ethyl acetate and the ammonium acetate solution from Sigma Aldrich (St. Louis, USA). Cell culture media (Minimal Essential Medium (MEM); Dulbecco's Modified Eagle Medium/F12 without phenol red (DMEM/F12); Roswell Park Memorial Institute 1640 medium (RPMI 1640)), penicillin streptomycin (P/S) solution, fetal bovine serum (FBS), charcoal-stripped FBS (CD-FBS), HEPES buffer, L-glutamine, bovine serum albumin (BSA) were purchased from Thermo Fisher Scientific Inc. (Waltham, USA). Zeocin® and Normocin® were obtained from Invivogen (San Diego, USA). Cell culture consumables were bought from Sarstedt AG + Co. KG (Nuembrecht, Germany), Carl Roth GmbH + Co. KG (Karlsruhe, Germany), and VWR International (Pennsylvania, USA). Lipopolysaccharide (LPS) from Escherichia coli, dexamethasone (Dexa), 17β-estradiol (E2), doxorubicin hydrochloride (Doxo), Anti-phospho-Histone H2A.X (Ser139) antibody (clone JBW301) and Tween-20®were acquired from Sigma Aldrich (St. Louis, USA). The 4',6-diamidine-2'-phenylindoledihydrochloride (DAPI) and the secondary antibody Alexa Fluor™ 633 F(ab')2 fragment of goat anti-mouse IgG(H+L) were purchased from Thermo Fisher Scientific Inc. (Waltham, USA). The CellTiter-Blue® reagent was acquired from Promega Corp. (Fitchburg, USA), formamidopyrimidine DNA glycosylase (FPG) enzyme from New England Biolabs (Frankfurt, Germany) and ethidium bromide and dimethyl sulfoxide (DMSO) from Carl Roth GmbH + Co. KG (Karlsruhe, Germany). Chemicals used for the preparation of buffers for the AIP assay were purchased from Carl Roth GmbH + Co. KG (Karlsruhe, Germany) and Sigma Aldrich (St. Louis, USA) and for the comet assay from Carl Roth GmbH + Co. KG (Karlsruhe, Germany) and Merck kGaA (Darmstadt, Germany). Low- and normal melting agarose were obtained from Bio-Rad Laboratories GesmbH (Vienna, Austria). Analytical standards of AOH, AME, ALT, ATX-I, TeA and TEN were purchased from Romer Labs (Tulln, Austria), while ALS

was acquired from Eubio, Andreas Köck e.U. (Vienna, Austria). The two mycotoxins isoALT and AA-III were synthesized at the Institute of Organic Chemistry at the Karlsruhe Institute of Technology in Germany (Altemöller et al., 2006; Nemecek et al., 2013), whereas ALTP was kindly provided by the Institute of Analytical Food Chemistry of the Technical University of Munich, Germany (Liu and Rychlik, 2015). ATX-II was previously isolated inhouse from fungal cultures grown on rice (Puntscher et al., 2019a). For cell culture experiments AOH was purchased from Sigma Aldrich (St. Louis, USA), TeA from Santa Cruz Biotechnology (Dallas, USA), ALTP from Cfm Oskar Tropitzsch (Marktredwitz, Germany), AME and ATX-I from Szabo-Scandic (Vienna, Austria), and AST from Molport (Riga, Latvia).

#### 2.2. Fractionation of the CE by RP-HPLC

The fractionation of the extract, originally obtained by Puntscher et al. (2019b) by growing the Alternaria alternata strain DSM 62010 on long rice, was performed according to the method previously described by Schwarz et al. (2012a), with some modifications. Briefly, the semi-preparative HPLC-system consisted of a Knauer Smartline 1000 (LPG) pump, a Knauer Manager 5000 controller (Knauer Wissenschaftliche Geräte GmbH, Berlin, Germany), and a six-way manual injection valve. For separation, a Phenomenex Luna column (250 mm imes21.2 mm, 5 µm) equipped with a Phenomenex SecurityGuard column (C18, 2 mm; Phenomenex Inc., Torrance, USA) was used. Detection was realized with an Agilent G1315D diode array detector (with a preparative flow cell; Agilent Technologies, Santa Clara, USA) at  $\lambda = 278$  nm. The instrument was operated with the ClarityChrom Software (Knauer Wissenschaftliche Geräte GmbH, Berlin, Germany), and data acquisition was achieved with the ChemStation analysis software (Agilent Technologies, Santa Clara, USA). As eluent A, water adjusted to pH 3 with formic acid was used, while eluent B consisted of a mixture of 90 % acetonitrile and 10 % water (v/v). For the fractionation, a binary gradient program with a constant flow rate of 7.5 ml/min was chosen. The program began with 19 % eluent B for 1 min, increased to 30 % B over 1 min, to 50 % B over the next 5 min, to 56 % B over 12 min, and then to 100 % B over 17 min, holding at 100 % B for 5 min. The gradient was then reset to the initial conditions in 2 min, followed by an additional 6 min of equilibration between runs. The extract was injected after resuspension in a 1:10 mixture of ethanol and eluent B, and a total of 27 fractions were manually collected. A representative chromatogram, recorded at a wavelength of  $\lambda = 278$  nm and showing the collection points, is presented in Supplementary Fig. S1.

The collected fractions were subjected to a liquid-liquid extraction with ethyl acetate to remove the water. Subsequently, the organic phase was evaporated to dryness using a SpeedVac system (Labconco Corp., Kansas City, USA and Vacuubrand GmbH + Co. KG, Wertheim, Germany). For cell culture experiments, the dried fractions were dissolved in DMSO at a concentration of 24 mg/ml. With the intention of minimizing the number of samples for the toxicological evaluation, selected single fractions (SF) with a similar mycotoxin profile (according to a preliminary qualitative LC-MS/MS analysis) were combined to obtain a total of eleven pooled fractions (F). The respective compositions are displayed in Fig. 2. All fractions obtained were stored at  $-80\,^{\circ}\text{C}$  until the time of analysis.

#### 2.3. Mycotoxin quantification by LC-MS/MS analysis

The quantification of the mycotoxins in the fractions was performed by LC-MS/MS according to the method developed by Puntscher et al. (2018). Briefly, the analysis was realized with a Sciex QTrap 6500+ LC-MS/MS system equipped with a Turbo-V<sup>TM</sup> electrospray ionization source (Sciex, Framingham, USA). MS data were acquired in multiple reaction monitoring mode, applying negative electrospray ionization. The analytes were separated on a Supelco Ascentis Express column (C18, 100 mm  $\times$  2.1 mm; 2.7  $\mu$ m, Merck kGaA, Darmstadt, Germany)

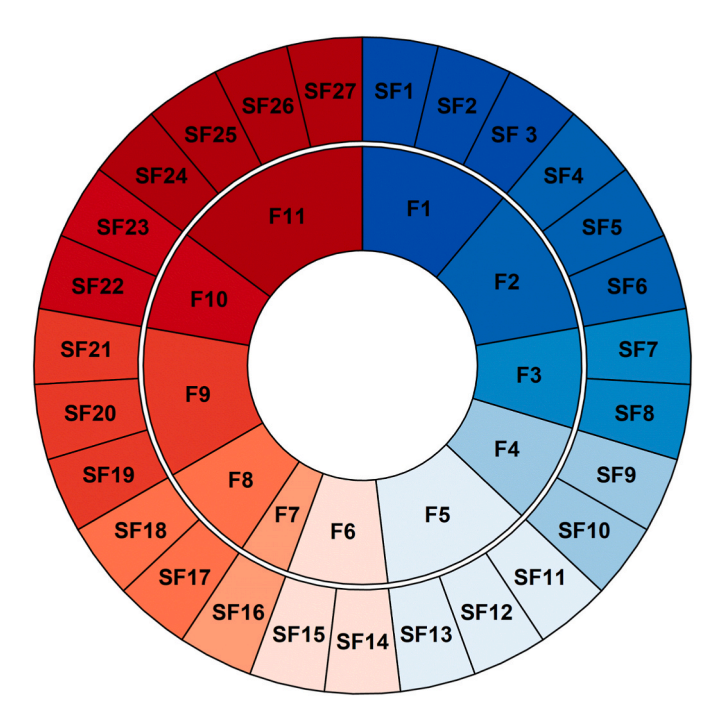


Fig. 2. Radial dendrogram showing the allocation of single fractions (SF1-SF27) to pooled fractions (F1-F11).

equipped with a Phenomenex SecurityGuard<sup>TM</sup> precolumn (C18, 2 mm; Phenomenex Inc., Torrance, USA), using an Agilent 1290 series UHPLC system (Agilent Technologies, Santa Clara, USA). Methanol served as eluent B, while eluent A consisted of a 5 mM ammonium acetate solution in water, with the pH adjusted to 8.7 using a 25 % ammonia solution. Before injection, the samples were diluted with a solvent consisting of 30 % methanol and 70 % LC-MS grade water  $(\nu/\nu)$ . As a blank, the methanol/water solution was used, and was injected after every calibration set and every fraction to avoid problems caused by carry-over. For quantification a multicomponent stock solution containing twelve *Alternaria* mycotoxins (AOH, AME, TEN, TeA, ALT, isoALT, ALS, AA-III, AST, ATX-I, ATX-II, ALTP) was prepared. Every fraction was measured in individually prepared triplicates. Data analysis was performed using the Skyline software (version 23.1).

#### 2.4. Preparation of Alternaria mycotoxin mixtures

To investigate the possible onset of combinatory effects, mixtures of multiple *Alternaria* mycotoxins were prepared in DMSO. The goal was to create mixtures that accurately reflect the mycotoxin profile of the fractions. Mycotoxins contained and identified in the mixtures (AOH, AME, TeA, AST, ATX-I, ATX-II and ALTP) were chosen based on their abundance in the fractions, the commercial availability, as well as the possibility to isolate the compounds in house. The specific composition of the mixtures with the respective concentrations of mycotoxins was based on the results of the LC-MS/MS analysis performed on the CE-fractions. Based on the activity of the fractions on the different toxicological endpoints, a total of ten mixtures corresponding to F3, F4, F6–F10, SF18, SF19 and SF22 were prepared and will in the following be referred to as M3, M4, M6-10, SM18, SM19 and SM22.

#### 2.5. Cell culture

THP1-Lucia<sup>TM</sup> monocytes (Invivogen, San Diego, USA) were routinely cultured in RPMI 1640 medium supplemented with 10 % heat inactivated FBS, 25 mM HEPES buffer, 1 % P/S (100 U/ml) and 100  $\mu$ g/ml Normocin®. To ensure the stability of the reporter gene, cells were grown under selection pressure by adding 100  $\mu$ g/ml of Zeocin® every second cell

passage. The human endometrial adenocarcinoma cell line Ishikawa was purchased from the European Collection of Authenticated Cell Cultures (ECACC) (Salisbury, UK). Cells were grown in MEM supplemented with 10 % heat inactivated FBS, 1 % Lglutamine and 1 % P/S (100 U/ml). The human hepatocarcinoma HepG2 cell line (ECACC; Salisbury, UK) was maintained in RPMI 1640 medium supplemented with 10% heat inactivated FBS and 1 % P/S (100 U/ml). All cells were kept in a humidified atmosphere at 37  $^{\circ}$ C and 5 % CO2 and were passaged twice per week when they reached approximately 80 % confluency. Screening for mycoplasma contamination took place at regular intervals.

#### 2.6. NF-κB reporter gene assay

To assess the impact on the NF-κB signaling pathway, the NF-κB reporter gene assay in THP1-Lucia<sup>TM</sup> monocytes was performed. In detail, cells were seeded into 96-well plates (0.1  $\times$  10<sup>6</sup> cells/well) and simultaneously incubated with the pooled CE-fractions (0.3–30  $\mu g/ml$ ), the mixtures corresponding to the highest concentration of the fractions, AST (0.01-25 µM), a solvent control (0.25% DMSO), and a negative control (1 µM Dexa) for 2 h. Afterwards, to activate the NF-kB signaling pathway and investigate the immunoinhibitory properties of the test compounds, 10 ng/ml LPS was added to the wells, and the cells were incubated for an additional 18 h. As positive control served LPS-treated cells (10 ng/ml). For the assessment of the immunostimulatory effects, LPS was only added to the wells of the positive and negative control. At the end of the incubation time (20 h), the NF-κB reporter gene assay was performed according to the manufacturer's protocol using Quanti-Luc (Invivogen, San Diego, USA), a coelenterazine-based luminescence reagent. The NF-κB activation was determined by measuring the luciferase activity with a microplate reader (Cytation 3 imaging plate reader) and the software Gen5 (version 3.08; BioTek Instruments, Winooski, USA).

#### 2.7. Alkaline phosphatase (AlP) assay

Potential estrogenic/antiestrogenic properties were investigated using the AlP assay in Ishikawa cells. Cells were seeded into 96-well plates  $(0.01 \times 10^6 \text{ cells/well})$  and allowed to grow for 48 h in assay medium (DMEM/F12 without phenol red supplemented with 5 % CD-FBS). Cells were subsequently incubated for 48 h in assay medium with the pooled CE-fractions (0.06-6 µg/ml), the mixtures corresponding to the highest concentrations of the fractions and AST (0.01–10  $\mu$ M). As a solvent control served 0.1 % DMSO, while 1 nM E2 was used as positive control. Cells were either co-incubated with 1 nM of E2 and the test substances/fractions to investigate antiestrogenic properties or exposed only to the test substances/fractions to assess estrogenic properties. Following the incubation, cells were washed thrice with phosphate buffered saline (PBS) and frozen at  $-80\,^{\circ}$ C for 20 min. To achieve lysis plates were thawed at room temperature for 5 min before the addition of 50 µl AlP buffer (5 mM 4-nitrophenylphosphate, 1 M diethanolamine, 0.24 mM MgCl<sub>2</sub>) per well. The absorbance was measured at  $\lambda = 405$  nm every 2 min for 1 h at 37 °C using a microplate reader and the Gen5 software. The slope of the curve in the linear range was used for the determination of the AlP activity.

#### 2.8. yH2AX assay

To assess genotoxic effects the  $\gamma H2AX$  assay in HepG2 cells was performed. The procedure for the  $\gamma H2AX$  assay followed the protocol published by Ebmeyer et al. (2019) with modifications as previously described by Crudo et al. (2024a). Briefly, HepG2 cells were seeded into clear bottom black 96-well plates (0.5  $\times$  10<sup>6</sup> cells/well) and grown for 24 h in growth medium. Afterwards, cells were treated with the single (120 µg/ml) and pooled (3–60 µg/ml) CE-fractions, the mixtures corresponding to the highest concentrations of the fractions, solvent control (0.5 % DMSO) and positive control (2.5 µM Doxo) for 4 h in assay medium (RPMI 1640 medium with 1 % P/S). Cells were fixed with ice-cold

methanol for 20 min at 4 °C. After cells were washed three times with PBS-T (PBS + 0.1 % Tween-20®), they were blocked for 1 h at room temperature with a blocking solution consisting of 1 % BSA in PBS-T. Cells were washed once with PBS-T, followed by incubation with the primary antibody solution (anti-phospho-Histone H2A.X (Ser139), clone JBW301; 1:400 in blocking solution) overnight at 4 °C. The next day, cells were washed thrice with PBS-T and incubated with the secondary antibody solution (Alexa Fluor<sup>TM</sup>633 F(ab')2 fragment of goat anti-mouse IgG(H + L); 1:500 in blocking solution) for 1 h at room temperature in the dark. Afterwards, cells were washed thrice with PBS-T, and the nuclei were stained with a 3  $\mu$ M DAPI solution (in PBS-T) for 30 min at room temperature in the dark. Finally, cells were washed again three times with PBS-T and plates were stored at 4 °C until analysis. Pictures were acquired with a BioTek Lionheart FX automated microscope (Agilent Technologies, Santa Clara, USA) equipped with the software Gen5. Fluorescence signals for DAPI were detected at 380/460 nm ( $\lambda_{ex}/\lambda_{em}$ ), and for  $\gamma$ H2AX at 620/655 nm ( $\lambda_{ex}/\lambda_{em}$ ). Two images per well were acquired from different optical fields. For each optical field at least 120 cells were scored, and the mean yH2AX signal intensities were normalized against the solvent control.

#### 2.9. Single-cell gel electrophoresis (comet assay)

The comet assay was carried out according to Tice et al. (2000), with some modifications. Briefly,  $0.35 \times 10^6$  HepG2 cells were seeded into 35 mm petri dishes and grown for 48 h. The cells were incubated with the single fractions (60 µg/ml SF18, SF19 and SF22, and 30 µg/ml SF19) and corresponding mixtures for 4 h in assay medium (RPMI 1640 medium with 1 % P/S). As positive controls, cells exposed for 1 min to UV-B radiation and cells exposed for 1 h to 50 μM H<sub>2</sub>O<sub>2</sub> were employed. As solvent control served 0.5 % DMSO. At the end of the incubation time, the cells were washed twice with PBS and detached with trypsin. Cell viability was determined through trypan blue exclusion test. Only samples with a cell viability above 80 % were further processed. For each condition, two times 30,000 cells were embedded in low-melting agarose onto a normal-melting agarose gel placed on a glass slide (two gel pads). In total two slides were prepared for each test condition. Both agarose solutions had a concentration of 0.8 % and were prepared in phosphate buffer (137 mM NaCl, 2.7 mM KCl, 1.5 mM KH<sub>2</sub>PO<sub>4</sub>, 8.1 mM Na<sub>2</sub>HPO<sub>4</sub>). Cell lysis was performed overnight at 4 °C by immersing the slides in a lysis buffer (10 % DMSO, 1 % Triton X-100 and 0.1 % lauroyl sarcosinate). One slide of each test condition was treated with FPG enzyme for 30 min at 37 °C to detect FPG-sensitive sites, which are indicative of oxidative DNA damage. All slides were equilibrated in the electrophoresis buffer (0.3 M NaOH, 1 mM EDTA) for 20 min, followed by electrophoresis at 300 mA for 20 min. Both equilibration and electrophoresis, were carried out on ice. The slides were subsequently washed with a neutralization buffer (TRIS, pH 7.5), and DNA was stained with a 0.02 mg/ml ethidium bromide solution. Image acquisition was achieved with a Zeiss Axioskop (Carl Zeiss AG, Oberkochen, Germany) at 546/590 nm ( $\lambda_{ex}/\lambda_{em}$ ), and the "Comet Assay IV" software (version 4.2.1; Perceptive Instruments, Suffolk, UK) was used for image analysis. In total, 50 cells per gel pad were scored for their tail intensity, resulting in 100 scores per biological replicate.

# 2.10. CellTiter-Blue® (CTB) assay

The CTB assay was carried out to determine potential cytotoxic effects in the applied cell models (THP1-Lucia<sup>TM</sup> monocytes, Ishikawa and HepG2 cells) to ensure that the effects observed in the other assays were not only artefacts due to cytotoxicity. For the assessment in THP1 cells, the monocytes were incubated under the same conditions as described for the NF- $\kappa$ B reporter gene assay (see section 2.6). After the incubation time ended, 20  $\mu$ l of the CTB reagent was added to each well (1:10 dilution) and cells were incubated for 2 h. The monocytes were centrifuged at 140 rfc for 2 min, and 100  $\mu$ l of the supernatants were

subsequently transferred to a black 96-well plate. Ishikawa and HepG2 were treated the same way as described for the AlP assay and the  $\gamma H2AX$  assay, respectively (see section 2.7 and 2.8). At the end of the incubation time, the test media were replaced with a 10 % CTB reagent solution (1:10 dilution in DMEM/F12 without phenol red for Ishikawa or DMEM without phenol red for HepG2 cells respectively). Cells were incubated for 50 min, followed by the transfer of 80  $\mu l$  of the supernatants to a black 96-well plate. For all cells the fluorescence measurement was conducted at 560/590 nm  $(\lambda_{ex}/\lambda_{em})$  with a microplate reader.

#### 2.11. Statistical analysis

Statistical analysis was performed with the Origin Pro® 2022 software (OriginLab, Northampton, USA). All cell culture-based experiments were performed in technical triplicates (or duplicates in the case of the comet assay) and in at least three biological replicates. Results were expressed as mean + standard deviation (SD) of the biological replicates and, depending on the endpoint, they were normalized to the respective positive or solvent controls (test over control, T/C). Student's *t*-test was performed to evaluate significant differences between the controls and the different test conditions or between the fractions and corresponding mixtures. One-way ANOVA with Fisher-LSD post-hoc test was conducted to determine differences between the various concentrations of the fractions.

#### 3. Results

# 3.1. Quantification of Alternaria mycotoxins in the single and pooled CE-fractions

The single and pooled CE-fractions were analyzed for twelve different *Alternaria* mycotoxins with an LC-MS/MS multi-method. The results of the quantification of mycotoxins in the pooled fractions (12 mg/ml) and in selected (relevant) single fractions (24 mg/ml) are reported in Table 1. A complete quantification of the single fractions is listed in Supplementary Table S1. For a clearer overview of the mycotoxin content in both pooled and single CE-fractions, the percentage distributions of the twelve *Alternaria* toxins are presented in Supplementary Fig. S2.

#### 3.2. Immunomodulatory effects

The assessment of the immunomodulatory effects was performed by applying the NF- $\kappa$ B assay in THP1-Lucia<sup>TM</sup> monocytes. In detail, three concentrations of the pooled CE-fractions (Fig. 2), namely 0.3, 3.0 and 30 µg/ml, were tested for their potential to inhibit the NF- $\kappa$ B pathway. As shown in Fig. 3A, all tested fractions suppressed the LPS-induced NF- $\kappa$ B pathway activation at the highest concentration tested (F1, F3–F11 – p < 0.001; F2 – p < 0.05). To exclude experimental artefacts deriving from cytotoxicity, the CTB assay was carried out in parallel. Data obtained only showed mild cytotoxicity following exposure of cells to 0.3 µg/ml of F3 and 30 µg/ml of F7, with a reduction of the signal to 87 % and 75 % respectively (p < 0.05 and 0.001; Fig. 3C).

Taking into consideration that all fractions contain multiple mycotoxins, the possible onset of combinatory effect was investigated. For this cause, the mixtures (M3, M4, M6-M10) corresponding to the highest concentrations of the most active fractions, namely 30  $\mu$ g/ml of F3, F4, F6–F10, were tested for their immunoinhibitory potential. The mycotoxins included in each mixture, as well as their respective concentrations, are depicted in Fig. 3E. The comparison of the NF- $\kappa$ B results obtained for the mixtures and the respective pooled fractions are shown in Fig. 3B. Unlike F3 and F4, the mixtures M3 and M4 were not able to reduce the LPS-induced luciferase signal and, therefore, significantly differed from the corresponding fractions (p < 0.001). As for M7 and M9, significant decreases in the luciferase signal were measured for the mixtures (p < 0.001), which, however, were more pronounced than the

**Table 1**Quantification of twelve *Alternaria* mycotoxins in the pooled CE-fractions (F) and in selected single fractions (SF).

Fractions						Concentrati	on [μM] <sup>a</sup>					
	AME	AOH	TEN	TeA	ALT	isoALT	ALS	AA-III	AST	ATX-I	ATX-II	ALTP
F1	≤0.01	<lod< td=""><td><lod< td=""><td>61</td><td><lod< td=""><td><lod< td=""><td><lod< td=""><td><lod< td=""><td>0.43</td><td>0.06</td><td><lod< td=""><td>0.06</td></lod<></td></lod<></td></lod<></td></lod<></td></lod<></td></lod<></td></lod<>	<lod< td=""><td>61</td><td><lod< td=""><td><lod< td=""><td><lod< td=""><td><lod< td=""><td>0.43</td><td>0.06</td><td><lod< td=""><td>0.06</td></lod<></td></lod<></td></lod<></td></lod<></td></lod<></td></lod<>	61	<lod< td=""><td><lod< td=""><td><lod< td=""><td><lod< td=""><td>0.43</td><td>0.06</td><td><lod< td=""><td>0.06</td></lod<></td></lod<></td></lod<></td></lod<></td></lod<>	<lod< td=""><td><lod< td=""><td><lod< td=""><td>0.43</td><td>0.06</td><td><lod< td=""><td>0.06</td></lod<></td></lod<></td></lod<></td></lod<>	<lod< td=""><td><lod< td=""><td>0.43</td><td>0.06</td><td><lod< td=""><td>0.06</td></lod<></td></lod<></td></lod<>	<lod< td=""><td>0.43</td><td>0.06</td><td><lod< td=""><td>0.06</td></lod<></td></lod<>	0.43	0.06	<lod< td=""><td>0.06</td></lod<>	0.06
F2	0.15	2.7	<lod< td=""><td>2100</td><td><lod< td=""><td><lod< td=""><td><lod< td=""><td><lod< td=""><td>0.61</td><td>11</td><td><lod< td=""><td>6.6</td></lod<></td></lod<></td></lod<></td></lod<></td></lod<></td></lod<>	2100	<lod< td=""><td><lod< td=""><td><lod< td=""><td><lod< td=""><td>0.61</td><td>11</td><td><lod< td=""><td>6.6</td></lod<></td></lod<></td></lod<></td></lod<></td></lod<>	<lod< td=""><td><lod< td=""><td><lod< td=""><td>0.61</td><td>11</td><td><lod< td=""><td>6.6</td></lod<></td></lod<></td></lod<></td></lod<>	<lod< td=""><td><lod< td=""><td>0.61</td><td>11</td><td><lod< td=""><td>6.6</td></lod<></td></lod<></td></lod<>	<lod< td=""><td>0.61</td><td>11</td><td><lod< td=""><td>6.6</td></lod<></td></lod<>	0.61	11	<lod< td=""><td>6.6</td></lod<>	6.6
F3	$\le$ 0.01	11	$\le$ 0.01	1300	0.04	<lod< td=""><td>0.46</td><td>0.15</td><td>0.33</td><td>32</td><td><lod< td=""><td>24</td></lod<></td></lod<>	0.46	0.15	0.33	32	<lod< td=""><td>24</td></lod<>	24
F4	0.02	0.16	<loq< td=""><td>260</td><td>0.28</td><td><lod< td=""><td>2.7</td><td>1.3</td><td>1.4</td><td>1.9</td><td><lod< td=""><td>23</td></lod<></td></lod<></td></loq<>	260	0.28	<lod< td=""><td>2.7</td><td>1.3</td><td>1.4</td><td>1.9</td><td><lod< td=""><td>23</td></lod<></td></lod<>	2.7	1.3	1.4	1.9	<lod< td=""><td>23</td></lod<>	23
F5	0.04	$\leq$ 0.01	$\leq$ 0.01	110	790	85	0.56	0.10	0.96	0.47	26	41
F6	0.03	0.06	20	300	1.1	0.10	71	1.3	0.54	2100	2.4	110
F7	$\le$ 0.01	68	0.02	65000	0.06	<loq< td=""><td>0.31</td><td>0.32</td><td>0.26</td><td>280</td><td>0.11</td><td>160</td></loq<>	0.31	0.32	0.26	280	0.11	160
F8	0.22	2.7	0.03	1400	3.5	<loq< td=""><td><lod< td=""><td><lod< td=""><td>24</td><td>14</td><td>5800</td><td>15</td></lod<></td></lod<></td></loq<>	<lod< td=""><td><lod< td=""><td>24</td><td>14</td><td>5800</td><td>15</td></lod<></td></lod<>	<lod< td=""><td>24</td><td>14</td><td>5800</td><td>15</td></lod<>	24	14	5800	15
F9	3.6	0.25	<loq< td=""><td>690</td><td>0.85</td><td><lod< td=""><td><lod< td=""><td><lod< td=""><td>2200</td><td>3.8</td><td>3700</td><td>13</td></lod<></td></lod<></td></lod<></td></loq<>	690	0.85	<lod< td=""><td><lod< td=""><td><lod< td=""><td>2200</td><td>3.8</td><td>3700</td><td>13</td></lod<></td></lod<></td></lod<>	<lod< td=""><td><lod< td=""><td>2200</td><td>3.8</td><td>3700</td><td>13</td></lod<></td></lod<>	<lod< td=""><td>2200</td><td>3.8</td><td>3700</td><td>13</td></lod<>	2200	3.8	3700	13
F10	$\le$ 0.01	0.14	<loq< td=""><td>460</td><td>0.15</td><td><lod< td=""><td><lod< td=""><td><lod< td=""><td>5300</td><td>1.5</td><td>18</td><td>2.2</td></lod<></td></lod<></td></lod<></td></loq<>	460	0.15	<lod< td=""><td><lod< td=""><td><lod< td=""><td>5300</td><td>1.5</td><td>18</td><td>2.2</td></lod<></td></lod<></td></lod<>	<lod< td=""><td><lod< td=""><td>5300</td><td>1.5</td><td>18</td><td>2.2</td></lod<></td></lod<>	<lod< td=""><td>5300</td><td>1.5</td><td>18</td><td>2.2</td></lod<>	5300	1.5	18	2.2
F11	≤0.01	0.08	<lod< td=""><td>98</td><td>0.05</td><td><lod< td=""><td><lod< td=""><td><lod< td=""><td>730</td><td>0.30</td><td>7.8</td><td>0.55</td></lod<></td></lod<></td></lod<></td></lod<>	98	0.05	<lod< td=""><td><lod< td=""><td><lod< td=""><td>730</td><td>0.30</td><td>7.8</td><td>0.55</td></lod<></td></lod<></td></lod<>	<lod< td=""><td><lod< td=""><td>730</td><td>0.30</td><td>7.8</td><td>0.55</td></lod<></td></lod<>	<lod< td=""><td>730</td><td>0.30</td><td>7.8</td><td>0.55</td></lod<>	730	0.30	7.8	0.55
SF17	0.08	2.0	0.01	2700	2.8	<lod< td=""><td><lod< td=""><td>0.13</td><td>17</td><td>18</td><td><lod< td=""><td>22</td></lod<></td></lod<></td></lod<>	<lod< td=""><td>0.13</td><td>17</td><td>18</td><td><lod< td=""><td>22</td></lod<></td></lod<>	0.13	17	18	<lod< td=""><td>22</td></lod<>	22
SF18	0.03	0.18	0.01	800	2.7	<lod< td=""><td><lod< td=""><td>0.08</td><td>83</td><td>17</td><td>1700</td><td>8.6</td></lod<></td></lod<>	<lod< td=""><td>0.08</td><td>83</td><td>17</td><td>1700</td><td>8.6</td></lod<>	0.08	83	17	1700	8.6
SF19	0.09	0.13	<loq< td=""><td>460</td><td>0.41</td><td><lod< td=""><td><lod< td=""><td>0.03</td><td>71</td><td>1.3</td><td>11000</td><td>7.9</td></lod<></td></lod<></td></loq<>	460	0.41	<lod< td=""><td><lod< td=""><td>0.03</td><td>71</td><td>1.3</td><td>11000</td><td>7.9</td></lod<></td></lod<>	<lod< td=""><td>0.03</td><td>71</td><td>1.3</td><td>11000</td><td>7.9</td></lod<>	0.03	71	1.3	11000	7.9
SF20	0.17	0.14	<loq< td=""><td>1600</td><td>0.74</td><td><lod< td=""><td><lod< td=""><td>0.06</td><td>120</td><td>5.6</td><td>610</td><td>21</td></lod<></td></lod<></td></loq<>	1600	0.74	<lod< td=""><td><lod< td=""><td>0.06</td><td>120</td><td>5.6</td><td>610</td><td>21</td></lod<></td></lod<>	<lod< td=""><td>0.06</td><td>120</td><td>5.6</td><td>610</td><td>21</td></lod<>	0.06	120	5.6	610	21
SF21	6.7	0.08	< 0.01	1500	0.53	<lod< td=""><td><lod< td=""><td>0.06</td><td>720</td><td>2.3</td><td>170</td><td>11</td></lod<></td></lod<>	<lod< td=""><td>0.06</td><td>720</td><td>2.3</td><td>170</td><td>11</td></lod<>	0.06	720	2.3	170	11
SF22	6.2	0.21	≤0.01	880	1.4	<lod< td=""><td><lod< td=""><td><lod< td=""><td>2400</td><td>1.6</td><td>34</td><td>5.0</td></lod<></td></lod<></td></lod<>	<lod< td=""><td><lod< td=""><td>2400</td><td>1.6</td><td>34</td><td>5.0</td></lod<></td></lod<>	<lod< td=""><td>2400</td><td>1.6</td><td>34</td><td>5.0</td></lod<>	2400	1.6	34	5.0
SF23	4.5	1.5	<lod< td=""><td>1100</td><td>0.91</td><td><lod< td=""><td><lod< td=""><td><lod< td=""><td>6500</td><td>7.0</td><td>11</td><td>9.5</td></lod<></td></lod<></td></lod<></td></lod<>	1100	0.91	<lod< td=""><td><lod< td=""><td><lod< td=""><td>6500</td><td>7.0</td><td>11</td><td>9.5</td></lod<></td></lod<></td></lod<>	<lod< td=""><td><lod< td=""><td>6500</td><td>7.0</td><td>11</td><td>9.5</td></lod<></td></lod<>	<lod< td=""><td>6500</td><td>7.0</td><td>11</td><td>9.5</td></lod<>	6500	7.0	11	9.5

AME: alternariol monomethyl ether, AOH: alternariol, TEN: tentoxin, TeA: tenuazonic acid, ALT: altenuene, isoALT: isoaltenuene, ALS: altenusin, AA-III: altenuic acid III, AST: altersetin, ATX-I: altertoxin-I, ATX-II: altertoxin-II, ALTP: alterperylenol.

immunosuppression observed for the corresponding fractions (p < 0.001). On the other hand, the suppressive effects caused by M10 (p < 0.001) were not as strong as the one of F10 and significant differences were seen (p < 0.001). When comparing the immunosuppressive effects of M6 and M8 to F6 and F8 respectively, no significant differences were observed. Surprisingly, the signals obtained from the CTB assay for M7-M9 were much lower than those of the fractions, suggesting more potent cytotoxicity arising from the exposure of THP1 monocytes to the mixtures (p < 0.001; Fig. 3D).

In addition to the immunoinhibitory effects, the pooled CE-fractions and respective mixtures were also tested for their potential to activate the NF- $\kappa$ B signaling pathway. As shown in Fig. 4A, incubation of the monocytes with 3 and 30  $\mu$ g/ml of F1 (p < 0.05) and 30  $\mu$ g/ml of F7, F9 and F10 (p < 0.001) resulted in an increase of the luminescence signal in the absence of LPS, indicating immunostimulatory effects. However, none of the mixtures lead to an increased luciferase expression and, therefore, the effects significantly differ from F7, F9 and F10, respectively (p < 0.001; Fig. 4B). As for the cytotoxicity testing (Supplementary Fig. S3) the results were comparable to those previously obtained for the experiments with LPS stimulation (Fig. 3C and D).

Considering the abundance of AST in the active fractions F9 and F10 (Table 1), it was tested for its immunomodulatory properties. Intriguingly, exposure of THP1 monocytes to the mycotoxin showed a concentration-dependent suppression of the LPS-induced NF- $\kappa B$  activation (Fig. 5A). The luminescence signal was significantly (p < 0.05) diminished starting from a concentration of 2  $\mu M$ . At the highest concentration tested, namely 25  $\mu M$ , the inhibitory effects caused by the mycotoxin even exceeded the ones of the negative control dexamethasone. At the same time, none of the tested concentrations caused a loss in cell viability (Fig. 5B). Furthermore, AST failed to activate the NF- $\kappa B$  pathway when the monocytes were exposed to the mycotoxin in the absence of LPS stimulation (Supplementary Fig. S4), thus proinflammatory effects could be excluded.

#### 3.3. Antiestrogenic effects

The CE-fractions, selected toxin mixtures, and AST were studied with respect to potential estrogenic and antiestrogenic effects in Ishikawa cells by applying the AlP assay. Ishikawa cells were exposed to CE fractions (0.06, 0.6 and  $6 \,\mu g/ml$ ) in the presence of 1 nM E2. In detail, all

fractions, except F1, F2, F5, and F11, showed significant differences to the positive control (1 nM E2) at the highest concentration (6  $\mu g/ml$ ) tested (p < 0.001). Furthermore, antiestrogenic effects could also be observed for 0.6  $\mu g/ml$  of F7 and F8 (p < 0.01 and p < 0.001; Fig. 6A). To contextualize the results with respect to cytotoxicity, also for this experimental workflow the CTB assay was carried out in parallel. According to the results in Fig. 6C, only the treatments with 6  $\mu g/ml$  of F7, F8, and F10 caused a significant decrease in cell viability (p < 0.001). However, the reductions observed for F8 and F10 were minor, and cell viability remained above 80 %. In addition, no induction of estrogenic stimuli could be observed for any of the fractions.

To elucidate whether combinations of selected Alternaria mycotoxins are responsible for the antiestrogenic properties exerted by the fractions, the mixtures M4 and M6-M10, corresponding to 6 µg/ml of the most active fractions F4 and F6-F10, were examined in the AlP assay. The composition of the mixtures with the respective concentrations of mycotoxins are depicted in Fig. 6E. Incubation with M4 or M6 did not result in a significant decrease of the E2-mediated induction of AlP activity. Therefore, the effects of the complementary fractions do not align with these results (p < 0.001; Fig. 6B). On the contrary, for the mixtures M7-M10, a reduction in the signal was detected (p < 0.001). Notably, although the changes in AlP activity observed for M7-M10 closely resemble those observed for the corresponding fractions, a significantly stronger suppression of AIP activity was measured for M7 and M9 as compared to the corresponding fractions F7 and F9 (p < 0.001). Moreover, F7, F8, M7 and M8 lead to significant decreases in viable cells (p < 0.001). However, the reduction caused by F8 and M8 remained above 80 % and the comparison of the results revealed no statistical differences in the effects resulting from the mixtures and the corresponding fractions

Considering the abundance of AST in the active fractions F9 and F10 (Table 1), the mycotoxin was tested in the AlP assay to assess its potential antiestrogenic effects and, consequently, to evaluate its contribution to the overall effects of the fractions and ultimately the CE. When AST was incubated in combination with 1 nM E2, significant decreases in the signal intensity were observed at concentrations  $\geq 5~\mu M$  (p < 0.001; Fig. 7A). The highest concentration tested, namely 10  $\mu M$  of AST, resulted in an almost complete suppression of the signal. The assessment of cytotoxicity with the CTB assay revealed a slight reduction of the signal at 10  $\mu M$  AST (p < 0.001), but cell viability remained above 80 %

<sup>&</sup>lt;sup>a</sup> Reported concentrations refer to the mycotoxin concentration in 12 mg/ml of pooled fractions (F) and 24 mg/ml of single fractions.

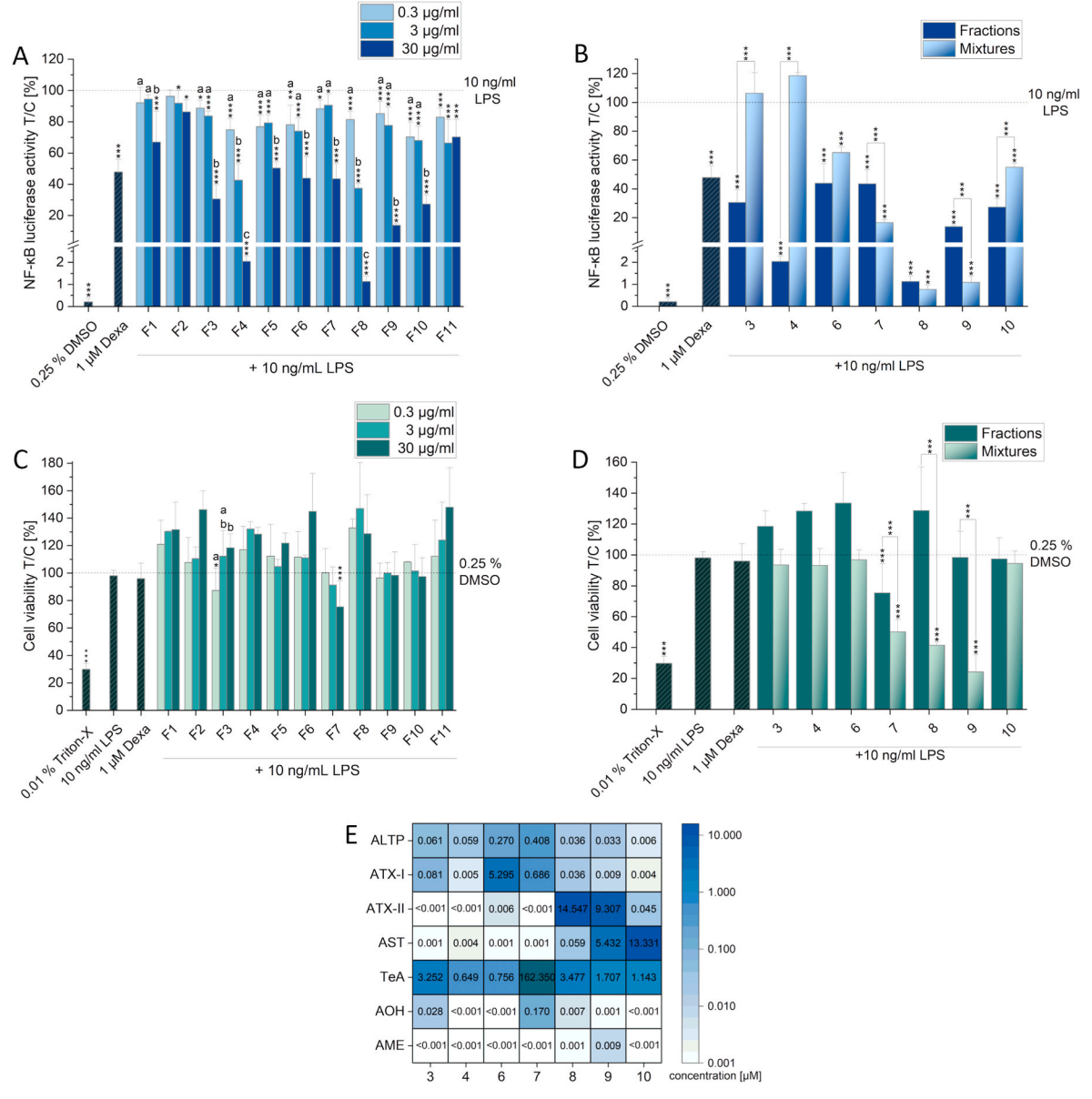


Fig. 3. Immunoinhibitory and cytotoxic impact of the pooled CE-fractions (0.3, 3 and 30 μg/ml) and selected *Alternaria* mycotoxin mixtures on THP1-Lucia<sup>TM</sup> monocytes. A) and B) report the results of the NF-κB reporter gene assay performed with simultaneous stimulation with 10 ng/ml lipopolysaccharide (LPS). As a negative control served 1 μM of dexamethasone (Dexa). C) and D) show the results of the CTB assay. As positive control for cytotoxicity served 0.01 % Triton X-100. B) and D) compare the effects of 30 μg/ml of the most active fractions with the corresponding mixtures. The values are displayed as means + SD of at least three independent experiments and in relation to the positive control (10 ng/ml LPS; A, B) or the solvent control (0.25 % DMSO; C, D; indicated as dotted lines). Significant differences between the treatments and the positive control (A, B) or the solvent control (C, D) and between the fractions and the mixtures (B, D) were calculated by applying the Student's t-test (\*p < 0.05, \*\*p < 0.01, and \*\*\*p < 0.001). Significant differences between the different concentrations of one fraction (A, C) were calculated with one-way ANOVA followed by a Fisher-LSD post hoc test (a-c; p < 0.05). In C) bars are only marked with a star (\*) when there are significant decreases in cell viability and in A) and C) additionally with letters only when there are significant differences between the groups. The heatmap in E) shows the concentrations in μM of the most abundant *Alternaria* mycotoxins in 30 μg/ml of the most active pooled fractions and corresponding mixtures.

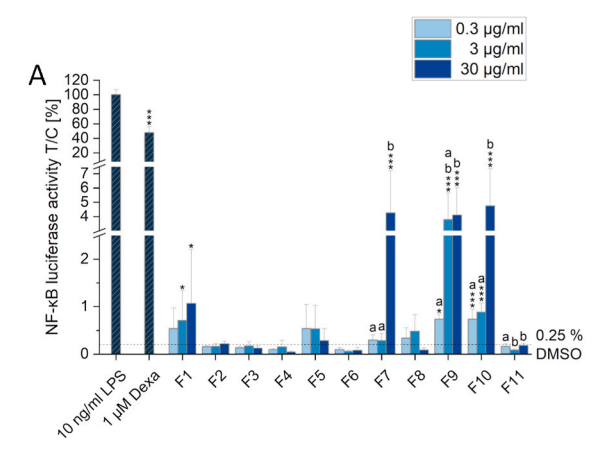
(Fig. 7B). The evaluation of the mycotoxin's estrogenic properties revealed no estrogenic activity (Supplementary Fig. S5).

#### 3.4. Genotoxic effects

#### 3.4.1. γH2AX assay

With the  $\gamma H2Ax$  assay the potential of the test compounds to induce double-strand breaks, through the quantification of the phosphorylated histone  $\gamma H2AX$  by fluorescence microscopy, can be assessed. To elucidate the impact of the different CE-fractions on the overall DNA damaging properties of the CE the  $\gamma H2AX$  assay was applied. Three concentrations of the pooled fractions (3, 30 and 60  $\mu g/ml)$  were tested

on HepG2 cell for their ability to induce the formation of phosphorylated histone  $\gamma H2AX$ . After 4 h incubation, significant increases in the fluorescence signal as compared to the solvent control (0.5 % DMSO) were observed for different concentrations of F1, F3 F5, F6 and F8–F10 (3 µg/ml F3, 3 µg/ml F5 - p < 0.01; 60 µg/ml F1 and F6, 3 µg/ml, 30 µg/ml and 60 µg/ml F8-10 – p < 0.001). The highest signals were measured for 30 and 60 µg/ml of F8–F10 (Fig. 8A). The results of the cytotoxicity testing showed slight but significant reductions in viability after exposure of the cells to 30 and 60 µg/ml of F7 and F10, and 60 µg/ml of F9 (p < 0.001). However, all signals remained above 80 % (Fig. 8C). Although some fractions caused significant formation of the phosphorylated histone  $\gamma H2AX$ , the effects of the active pooled fractions



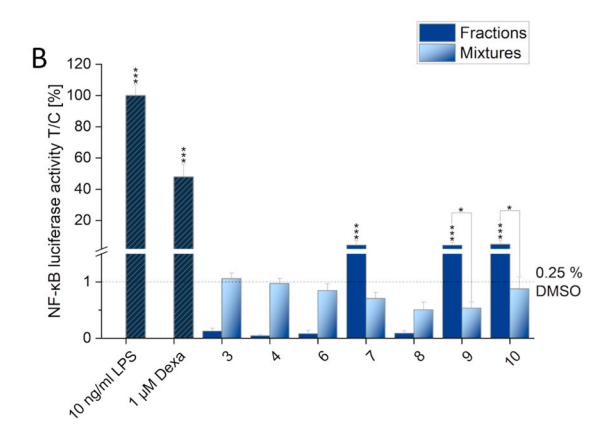
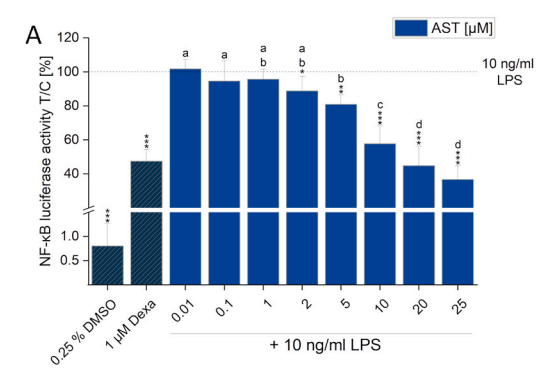


Fig. 4. Immunostimulatory impact of the pooled CE-fractions (0.3, 3 and 30 μg/ml) and selected *Alternaria* mycotoxin mixtures on THP1-Lucia<sup>TM</sup> monocytes. A) reports the results of the NF-κB reporter gene assay while in B) the comparison between 30 μg/ml of the most active fractions and the corresponding mixtures is shown. As a negative control served 1 μM of dexamethasone (Dexa). The values are displayed as means + SD of at least three independent experiments and in relation to the solvent control (0.25 % DMSO; indicated as dotted line) after normalization to the positive control (10 ng/ml LPS). Significant differences between the treatments and the solvent control (A, B) and between the fractions and the mixtures (B) were calculated by applying the Student's *t*-test (\*p < 0.05, \*\*p < 0.01, and \*\*\*p < 0.001). Significant differences between the different concentrations of one fraction (A) were calculated with one-way ANOVA followed by a Fisher-LSD post hoc test (ab p < 0.05).



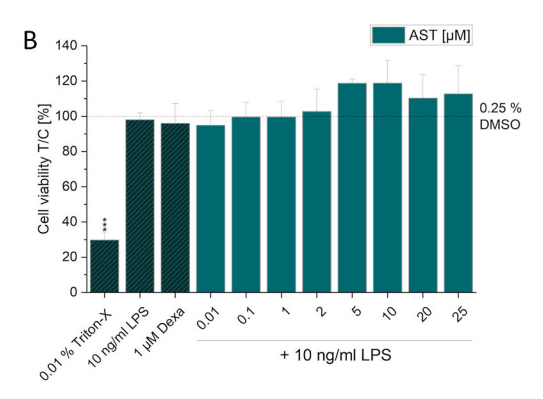


Fig. 5. Immunosuppressive and cytotoxic impact of AST  $(0.01-25 \,\mu\text{M})$  on THP1-Lucia<sup>TM</sup> monocytes. A) reports the results of the NF-kB reporter gene assay performed with simultaneous stimulation with 10 ng/ml lipopolysaccharide (LPS). As a negative control served 1  $\mu$ M of dexamethasone (Dexa). B) shows the results of the CTB assay and as a positive control for cytotoxicity served 0.01 % Triton X-100. The values are displayed as means + SD of at least three independent experiments and in relation to the positive control (10 ng/ml LPS; A) or the solvent control (0.25 % DMSO; B), which are indicated as dotted lines. Significant differences between the samples and the positive control (A) or the solvent control (B) were calculated by applying the Student's *t*-test (\*p < 0.05, \*\*p < 0.01, and \*\*\*p < 0.001). Significant differences between the different concentrations were calculated with one-way ANOVA followed by a Fisher-LSD post hoc test (a-d; p < 0.05). In B) bars are only marked with a star (\*) when there are significant decreases in cell viability and additionally with letters when there are significant differences between the concentrations.

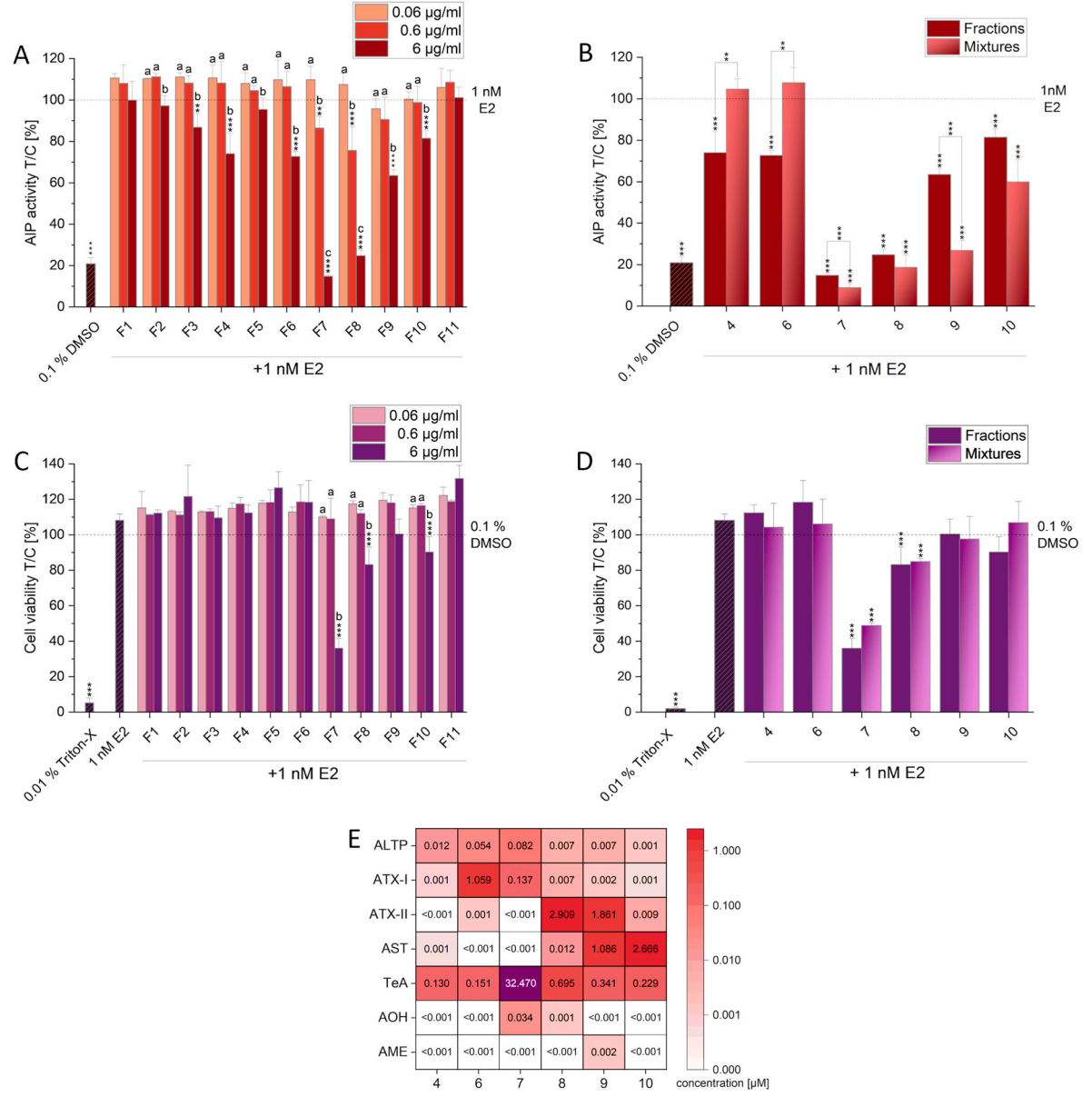
at different concentrations were quite similar and the signal intensities remained modest. In order to possibly see greater differences in the effects between different active fractions at higher signal intensities, the single fractions were also examined at the highest possible concentration, namely 120 µg/ml. In Fig. 8A, a selection of the results of the single fractions (SF17-SF23), of which the most active pooled fractions F8–F9 (Fig. 2) are composed of, are shown. Amongst the genotoxic single fractions SF18, SF19 and SF22 were found to be the most potent (p < 0.001). It must be pointed out that all tested single fractions led to a slight decrease in cell viability, but signals remained above 80 % (SF17-22 - p < 0.001, SF23 - p < 0.05). An exception was SF19, which resulted in a 25 % reduction in viability (p < 0.001; Fig. 8C). The results of all single fractions tested in the  $\gamma$ H2AX assay and the CTB assay are reported in Supplementary Fig. S6.

To investigate the contribution of combinatory effects on genotoxicity exerted by the different fractions, the mixtures M8-M10 (corresponding to 60  $\mu g/ml$  of F8–F10), and SM18, SM19 and SM22 (corresponding to 120  $\mu g/ml$  of SF18, SF19 and SF22) were tested. The composition of the mixtures with the respective concentrations of

mycotoxins are depicted in Fig. 8F. Incubation of HepG2 cells for 4 h resulted in a significant increase in  $\gamma H2AX$  expression for all mixtures tested (M8, M9, SM18 – p <0.001, M10 – p <0.01, SM22 – p <0.05; Fig. 8B). However, significant differences in the fluorescence intensity between F8/M8, F9/M9, SF18/SM18 and SF19/SM19 (p <0.001) were observed. While M8, M9 and SM19 resulted in stronger genotoxicity than the corresponding fractions, the effects caused by SM18 were not as strong as the one observed for SF18. On the contrary, signals measured for F10/M10 and SF22/SM22 were not found to be statistically different. Moreover, in contrast to some of the fractions, none of the mixtures resulted in a reduction of viable cells during the assessment of cytotoxicity with the CTB assay. However, significant differences between SF19/SM19 and SF22/SM22 (p <0.001) were observed (Fig. 8D). Representative fluorescence images of the controls, SF19 and SM19 are reported in Fig. 8E.

#### 3.4.2. Comet assay of single CE-fractions and mixtures

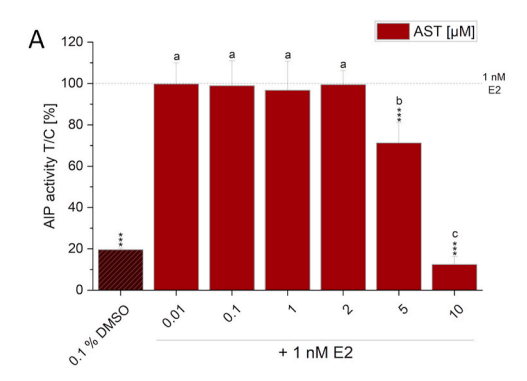
To further characterize the genotoxic properties of the most active fractions and corresponding mixtures identified in the  $\gamma$ H2AX assay (see



**Fig. 6.** Antiestrogenic and cytotoxic impact of the pooled CE-fractions (0.06, 0.6 and 6 μg/ml) and selected *Alternaria* mycotoxin mixtures on Ishikawa cells. A) and B) report the results of the AlP assay performed with simultaneous incubation with 1 nM 17β-estradiol (E2). C) and D) show the results of the CTB assay. As a positive control for cytotoxicity served 0.01 % Triton X-100. B) and D) compare the effects of 6 μg/ml of the most active fractions with the corresponding mixtures. The values are displayed as means + SD of at least three independent experiments and in relation to the positive control (1 nM E2; A, B) or the solvent control (0.1 % DMSO; C, D), indicated as dotted lines. Significant differences between the treatments and the positive control (A, B) or the solvent control (C, D) and between the fractions and the mixtures (B, D) were calculated by applying the Student's *t*-test (\*p < 0.05, \*\*p < 0.01, and \*\*\*p < 0.001). Significant differences between the different concentrations of one fraction (A, C) were calculated with one-way ANOVA followed by a Fisher-LSD post hoc test (a-c; p < 0.05). In C) bars are only marked with a star (\*) when there are significant decreases in cell viability and in (A and C) additionally with letters only when there are significant differences between the groups. The heatmap in E) shows the concentrations in μM of the most abundant *Alternaria* mycotoxins in 6 μg/ml of the most active pooled fractions and corresponding mixtures.

section 3.4.1) their potential to induce single and double-strand DNA breaks, as well as alkali-labile sites, was investigated by applying the comet assay both in the presence and absence of FPG enzyme. Since incubation of HepG2 cells with 120  $\mu$ g/ml of SF19 resulted in a reduction in cell viability below 80 % in trypan blue exclusion test, only 60  $\mu$ g/ml of all test solutions were applied. As shown in Fig. 9A, the single fractions SF18, SF19 and SF22 significantly induced DNA-strand breaks (p < 0.001), measured as tail intensity, after 4 h incubation as compared to the solvent control (0.5 % DMSO). Furthermore, FPG treatment significantly increased the DNA damage for SF18 (p < 0.01) and SF22 (p < 0.05). However, during the scoring of the nuclei of cells exposed to 60

 $\mu g/ml$  of SF19, only ghost cells could be detected. These cells are characterized by a small/absent nucleoid head with a long tail and, since the DNA is strongly damaged, a proper scoring cannot be achieved (Hong et al., 2020). For this reason, 30  $\mu g/ml$  of SF19 was additionally tested to correctly score the nuclei. For this concentration proper scoring could be realized and in addition to an increase in genotoxicity (without and with FPG – p<0.01) significant differences between the treatment without and with FPG were observed (p < 0.005). With regards to the results obtained for the mixtures, SM18 and SM19 followed a similar pattern as the corresponding fractions. In detail, the incubation of HepG2 cells with 60  $\mu g/ml$  of SM19 also resulted in the formation of



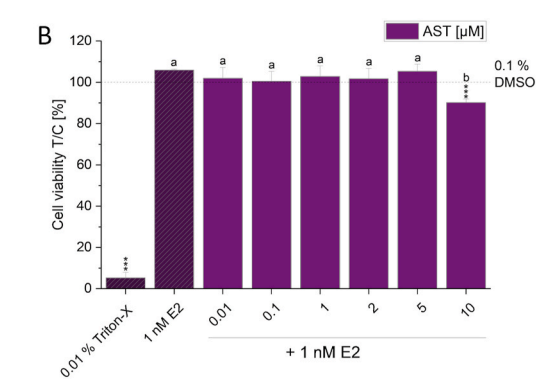


Fig. 7. Antiestrogenic and cytotoxic impact of AST  $(0.01-10~\mu\text{M})$  on Ishikawa cells. A) reports the results of the AIP assay performed with simultaneous incubation with 1 nM  $17\beta$ -estradiol (E2). B) shows the results of the CTB assay. As a positive control for cytotoxicity served 0.01 % Triton X-100. The values are displayed as means + SD of at least three independent experiments and in relation to the positive control (1 nM E2; A) or the solvent control (0.1 % DMSO; B) indicated as dotted lines. Significant differences between the samples and the positive control (A) or the solvent control (B) were calculated by applying the Student's t-test (\*p < 0.05, \*\*p < 0.01, and \*\*\*p < 0.001). Significant differences between the different concentrations were calculated with one-way ANOVA followed by a Fisher-LSD post hoc test (a-c; p < 0.05).

ghost cells and the signals could therefore only be considered as an approximation. However, treatment with 60  $\mu g/ml$  of SM18 and 30  $\mu g/ml$  of SM19 resulted in significant and scorable increases in tail intensities as compared to the solvent control (p < 0.001) and the obtained results do not statistically differ from the ones of the respective fractions. Moreover, treatment with FPG enzyme led to a further and statistically significant increase in tail intensity (p < 0.05). On the contrary, exposure of the cells to 60  $\mu g/ml$  of SM22 without FPG did not lead to any DNA damage. However, an increase in the signal was observed when FPG-treatment was applied (p < 0.001). Moreover, all signals obtained for SM22 differ significantly from the ones of SF22 (p < 0.001). In detail, while SF22 caused genotoxicity (p < 0.005; with and without FPG treatment), for SM22 only minor increases in tail intensity (p < 0.05) could be observed when FPG enzyme was added. Representative images of cells exposed to various treatments are reported in Fig. 9B.

#### 4. Discussion

Species within the Alternaria genus are recognized for their production of several secondary metabolites, including a diverse array of mycotoxins. Previous studies have explored various adverse effects associated with these toxins, with research focusing mainly on individual compounds, thereby often limited by commercial availability. Notably, it was observed that multiple mycotoxins can contaminate a single food commodity simultaneously, potentially leading to combined bioactivities. These combinatory effects depend on the specific composition and concentration of the toxin mixtures (Crudo et al., 2019). To accurately assess the risks posed by exposure to this group of structurally diverse molecules, the evaluation of further data on both, individual and combined effects, is essential. Therefore, the aim of this study was to fractionate a complex Alternaria mycotoxin extract to identify the individual compounds or combinations of toxins responsible for the overall immunomodulatory, antiestrogenic and genotoxic effects of a complex Alternaria alternata extract (Aichinger et al., 2019; Crudo and Partsch et al., 2024).

First, the fractions, which had a less complex composition compared to the original extract, were amongst others tested for their immuno-modulatory properties. As shown in Fig. 3A, co-incubation of THP1-Lucia<sup>TM</sup> monocytes with the different fractions and LPS resulted in a reduced luciferase activity, suggesting immunoinhibitory properties. Furthermore, the exposure of the cells to some of the fractions without adding LPS lead to an activation of the NF-κB signaling pathway (Fig. 4A). These results are in accordance with previously published results where a different set of fractions obtained by supercritical fluid chromatography (SFC) was investigated. Based on the results of the LC-

MS/MS analysis (Table 1), none of the known immunosuppressive Alternaria mycotoxins that could be quantified in the fractions, namely AOH, AME, ATX-I, ATX-II and ALTP, can individually account for the observed effects. This is because their concentrations in the tested fractions were far below the levels previously reported to exert immunosuppressive effects (Crudo and Partsch et al., 2024; Del Favero et al., 2020; Kollarova et al., 2018). Moreover, although TeA is present in all the fractions, it can be ruled out as the cause of the overall effects, as Crudo and Partsch et al. (2024) demonstrated that it does not exhibit immunosuppressive effects up to a concentration of 250 µM. Hence, mixtures corresponding to the most active fractions in terms of composition and concentration of mycotoxins were prepared and tested for their immunomodulatory properties (Fig. 3B). Except for M3 and M4, all mixtures exerted immunosuppressive effects and followed a similar pattern as the correlating fractions. Notably, the comparison between the effects exerted by F6/M6 and F8/M8 showed no significant differences. This suggests that the suppression of the NF-κB pathway observed after exposure of cells to these fractions was likely due to combinatory effects of the known mycotoxins present. To rule out that the reduced signal in the NF-κB reporter gene assay was not only due to a loss in viable cells, the CTB assay was carried out under the same conditions (Fig. 3C and D). The results of the assessment of cell viability revealed significant differences between F7–F9 and M7-M9 respectively. with the mixtures causing greater cytotoxicity than the related fractions. One plausible explanation could be the more complex composition of the fractions and the presence of unknown compounds (Crudo and Partsch et al., 2024).

Unlike the corresponding mixtures, F7, F9 and F10 also exerted immunostimulatory effects (Fig. 4A). The NF-κB transcription factor is involved in various cellular processes, including immune responses, inflammation, and apoptosis. Its role on the regulation of apoptosis is quite complex and context dependent. Several studies could demonstrate, that the inhibition of the NF-kB pathway leads to apoptosis in THP1 cells, while NF-kB activation can support survival pathways (Bai et al., 2013; Lee et al., 2007; Park and Kim, 2013). The unknown immunostimulatory compounds, which are only present in the fractions, might stimulate the expression of pro-survival factors and anti-apoptotic genes, thus preventing cell death. The fact that only the fractions act as immunostimulants also underpins the assumption that unknown Alternaria mycotoxins or other active compounds are present in the CE. Since the extract represents a natural product, the co-occurrence of additional secondary metabolites like allergens seems plausible. The most relevant Alternaria alternata allergen is Alt a 1, a small protein associated with Alternaria-induced asthma. Among all Alternaria alternata allergens it serves as a main compound to induce initial allergic

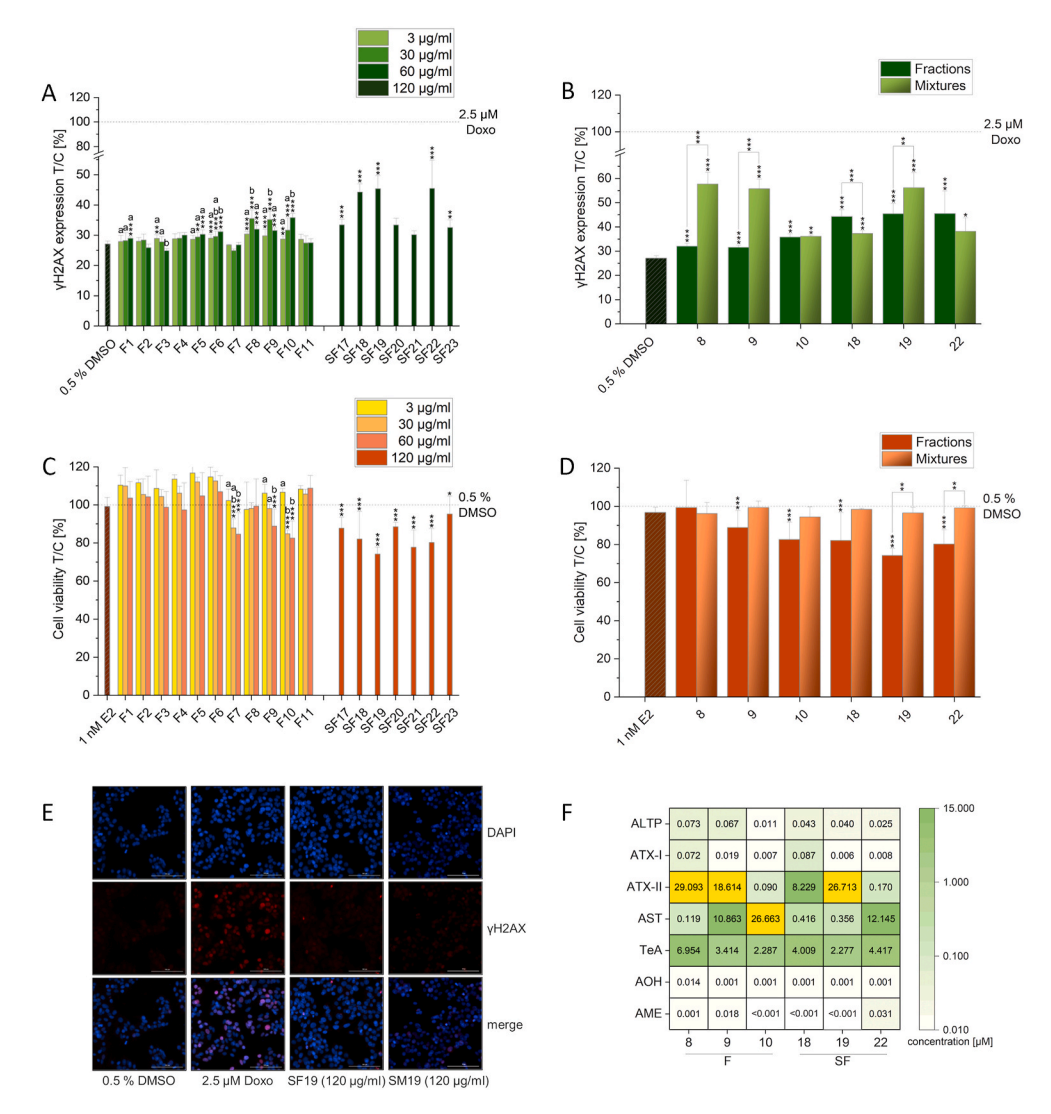


Fig. 8. Genotoxic and cytotoxic impact of the pooled CE-fractions (0.3, 3 and 30  $\mu$ g/ml), the single CE-fractions (120  $\mu$ g/ml) and selected *Alternaria* mycotoxin mixtures on HepG2 cells. A) and B) report the results of the  $\gamma$ H2AX assay. C) and D) show the results of the CTB assay. B) and D) compare the effects of 60  $\mu$ g/ml and 120  $\mu$ g/ml of the most active pooled and single fractions respectively with the corresponding mixtures. The values are displayed as means + SD of at least three independent experiments and in relation to the positive control (2.5  $\mu$ M doxorubicin (Doxo; A, B) or the solvent control (0.5 % DMSO; C, D), indicated as dotted lines. Significant differences between the treatments and the positive control (A, B) or the solvent control (C, D) and between the fractions and the mixtures (B, D) were calculated by applying the Student's *t*-test (\*p < 0.05, \*\*p < 0.01, and \*\*\*p < 0.001). Significant differences between the different concentrations of one fraction (A, C) were calculated with one-way ANOVA followed by a Fisher-LSD post hoc test (a-b p < 0.05). In C) bars are only marked with a star (\*) when there are significant decreases in cell viability and in A) and C) additionally with letters only when there are significant differences between the groups. In E) representative fluorescence images of the nuclei (blue),  $\gamma$ H2AX (red) and the merged channels are depicted. The heatmap in F) shows the concentrations in  $\mu$ M of the most abundant *Alternaria* mycotoxins in 60 and 120  $\mu$ g/ml of the most active pooled and single fractions respectively and corresponding mixtures. (For interpretation of the references to colour in this figure legend, the reader is referred to the Web version of this article.)

sensitization. Of note, research has demonstrated that Alt a 1 triggers the NF- $\kappa$ B pathway in THP1 monocytes through interaction with TLR4 (Hernandez-Ramirez et al., 2022). However, the presence of the allergen in the fractions as well as its possible contribution to the observed effects need to be verified in dedicated studies in the future.

Since two of the most active fractions (i.e. F9 and F10) were found to contain high concentrations of AST (5 and 13  $\mu M$ , respectively; Fig. 3E), the mycotoxin was tested singularly for its immunomodulatory properties. The results demonstrate the potency of AST to suppress LPS-induced NF- $\kappa B$ -induction in the absence of cytotoxicity (Fig. 5A and B). However, the reduction of the signal in the NF- $\kappa B$  assay to 80 % at 5  $\mu M$  and the supposedly reduction to around 55 % at 13  $\mu M$  were still above the effects caused by the two fractions. Conclusively, it can be assumed that AST is likely to contribute to the immunosuppressive effects of the fractions but is not solely responsible. To the best of our knowledge, this is the first time

that AST has been described as an immunosuppressive compound *in vitro*. Future *in vivo* studies are essential to validate these findings and offer a more comprehensive understanding of the immunosuppressive effects of this mycotoxin. Of note, this unique *Alternaria* mycotoxin shares, amongst others, structural similarities with the *Fusarium* toxin equisetin and the tetramic acid derivative trichosetin (Marfori et al., 2002; Vesonder et al., 1979). In this context, our findings show commonalities with a study carried out by Qin et al. (2015), who showed that proliferatin A-C, analogues of trichosetin, suppress inflammation through the inhibition of translocation of the NF-κB/p65 subunit to the nucleus and the modulation of phosphorylation of various regulatory proteins. However, since this only provides an insight into the possible mode of action of the structurally related compound AST, further research is required to elucidate the exact molecular mechanisms involved in the immunosuppressive properties of this *Alternaria* mycotoxin.

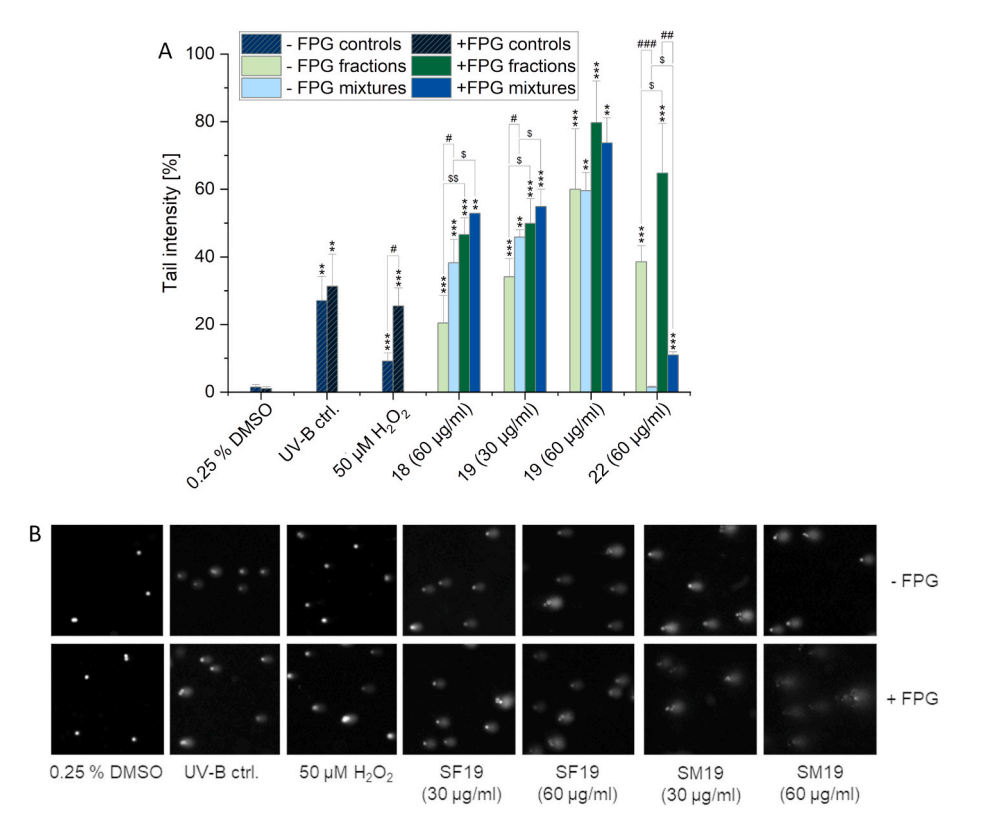


Fig. 9. DNA-damaging impact of the single CE-fractions SF18 (60  $\mu$ g/ml), SF19 (30, 60  $\mu$ g/ml) and SF22 (60  $\mu$ g/ml) and the correlating mixtures on HepG2 cells, measured in the comet assay. A) reports the tail intensities detected after exposure of HepG2 cells to the various test conditions for 4 h. As positive controls served 1 min exposure to UV-B irradiation and treatment with 50  $\mu$ M  $H_2O_2$  for 60 min. Light and dark bars indicate treatments without or with formamidopyrimidine-DNA glycosylase (FPG) enzyme, respectively. The Student's *t*-test was applied to calculate significant differences between the treatments and the solvent control (0.5 % DMSO; \*p < 0.05, \*\*p < 0.01, and \*\*\*p < 0.001), between treatment with and without FPG (\$p < 0.05, \$\$p < 0.01, and \$\$\$p < 0.001), and between the fractions and the corresponding mixtures (#p < 0.05, #p < 0.01, and ###p < 0.001). In B) representative fluorescence images of nuclei of cells exposed to the controls, SF19 and SM19 are displayed.

The Alternaria alternata extract used in the present study was previously described to suppress the E2-induced activation of the ER signaling pathway (Aichinger et al., 2019). So far, only ALTP and ATX-I have been identified as minor contributors to the overall effects, but a full elucidation has not yet been possible (Crudo and Partsch et al., 2024). In agreement with Aichinger et al. (2019) reported for the CE, and Crudo and Partsch et al. (2024) for the SFC set of fractions, antiestrogenic activity was observed for some of the fractions in the present study (Fig. 6A). Although the two known antiestrogenic mycotoxins ALTP and ATX-I were present in the most active fractions F4 and F6-F10, the LC-MS/MS analysis revealed that the levels were below the active concentrations of 0.4 and 2 µM respectively (Fig. 6E) previously reported by Crudo and Partsch et al. (2024). Also in this case TeA cannot be held responsible since it was previously shown to not possess any antiestrogenic properties (Aichinger et al., 2019). Furthermore, the high levels of ATX-II in fractions F8 and F9 suggest that this mycotoxin may significantly contribute to the observed effects of these fractions. However, a previous study by Aichinger et al. (2019) found no significant differences between the antiestrogenic effects of the complex extract (CE) and those of a reduced extract, from which ATX-II and STTX-III were removed. These findings imply that ATX-II is unlikely to be the primary compound responsible for these effects. Nevertheless, further experimental validation is needed to confirm this hypothesis. Because the overall effects cannot be explained by the presence of a known single compound, the mixtures consisting of the most abundant seven mycotoxins, and corresponding to the treatments with 6 µg/ml of the pooled fractions, were tested in the AlP assay to investigate the possible onset of combinatory effects. Thereby for M4 and M6, the effects differed from the ones of the correlating fractions (Fig. 6B) and, therefore, the mixtures - or rather mixture toxicology – do not provide an explanation for the effects exerted by the fractions. On the contrary, the signal intensities measured for M7-M10 followed a similar pattern as for the respective fractions (F7–F10). In addition, comparison of the CTB assay results between the fractions and the mixtures revealed no differences in signal intensities (Fig. 6D). Thus, the antiestrogenic properties of these four fractions appear to be primarily due to the combined toxicity of seven different *Alternaria* mycotoxins.

Since the AST-containing fractions F9 and F10 were also among the most active in the AlP assay, AST was tested for its estrogenic and antiestrogenic potential. The results showed the ability of AST in noncytotoxic concentrations to potently counteract the estrogenicity of E2 (Fig. 7A and B). These results support the characterization of AST as a novel antiestrogenic factor in natural Alternaria mycotoxin mixtures. However, to fully confirm these findings and gain a deeper understanding of the actual impact of this mycotoxin on the ER-pathway, further in vivo studies are required. With regards to the underlying mechanisms, in this case only limited data exists. However, one plausible mechanism involves the activation of the aryl hydrocarbon receptor (AhR)/AhR nuclear translocator (ARNT) pathway. The AhR can be activated by molecules with a planar structure, such as steroids (Hu et al., 2007). As for the metabolization of estrogens, it is known that there are several cytochrome P450 (CYP) enzymes involved. The activation of the AhR may lead to an induction of target genes (e.g. CYP1A1 gene) (Tsuchiya et al., 2005), as well as the inhibition of the expression of E2-responsive genes, followed by the degradation of E2 and the facilitated ubiquitination and proteasomal degradation of the ER, as suggested by Suchar et al. (1996) andWormke et al. (2000, 2003). Despite no information about the ability of AST to activate the AhR is

currently available, some Alternaria mycotoxins (i.e. AOH, ATX-I and ATX-II) were previously reported to activate the receptor (Hohenbichler et al., 2020). This activation, in turn, induces the transcription of CYP1A1, which then also plays a crucial role in the metabolism of these mycotoxins (Pahlke et al., 2016; Schreck et al., 2012). It should be noted that, despite Aichinger et al. (2019) demonstrated the ability of CE to activate the AhR/ARNT signaling pathway and strongly induce the transcription of CYP1A1, this activation did not lead to any enhancement in E2 degradation. Ultimately, the molecular mechanisms of AST remain uncertain, and more research is needed to clarify if the mycotoxin can induce the CYP1A1-catalysed degradation of E2 and/or the ERs through the activation of the AhR/ARNT signaling pathway. Of note, Groestlinger et al. (2022) demonstrated that AOH reduces the nuclear translocation of the NF-κB/p65 subunit while also increasing the AhR mobilization, thus suggesting that the AhR and the known crosstalk between these two pathways might play a role in the immunoinhibitory effects of some Alternaria mycotoxins. Since the applied CE and almost all the fractions possess immunosuppressive as well as antiestrogenic properties, it might be speculated that the effects on these pathways are interlinked by AhR-activation effects.

With respect to genotoxicity of complex *Alternaria* toxin mixtures, the epoxide-bearing pervlene quinone ATX-II has been identified as a potent mutagen, exceeding by far the genotoxic properties of AOH and AME. (Fleck et al., 2012; Pfeiffer et al., 2007; Schwarz et al., 2012a, 2012b). When investigating the genotoxicity of a natural Alternaria mycotoxin extract, Schwarz et al. (2012b) identified ATX-II and STTX-III as important contributors to the overall effect. Indeed, both mycotoxins were found to be present in the CE investigated in the present study, but the genotoxic potency of the complex extract exceeded the expected impact of these two perylene quinones, thus arguing for additional genotoxic components still to be identified (Aichinger et al., 2019). AOH and AME were shown to induce the formation of γH2AX in HepG2 cells, but only at  $100 \mu M$  (Hessel-Pras et al., 2019). In the comet assay the DNA-strand breaking potency of these two compounds seems to be cell line dependent. For example, the active concentration of AOH ranges from 1  $\mu M$  in A431 and HT-29 cells to 30 µM in RAW 264.7 cells (Fehr et al., 2009; Solhaug et al., 2012), and for AME from 1  $\mu$ M in A431 cells to 10  $\mu$ M in HT-29 cells (Fehr et al., 2009). These concentrations are far above the ones present in the CE and the different fractions tested in the present study (Table 1) (Aichinger et al., 2019). Thus, in this study the potential contribution of combinatory genotoxic effects was investigated. In the γH2AX assay, only F10/M10 and SF22/SM22 did not significantly differ from each other, suggesting that the combinations of mycotoxins tested are likely responsible for the effects exerted by these fractions (Fig. 8B). Crudo et al. (2024a) recently reported that ATX-II does not trigger yH2AX formation in HepG2 cells and suggested that AOH might inhibit the kinases responsible for γH2AX formation. Since both mycotoxins are present in the active fractions, their genotoxicity was also assessed in the comet assay (Fig. 9). As reported in Fig. 2, amongst others F8 consists of SF18, F9 of SF19 and F10 of SF22. Since these three single fractions caused the strongest genotoxicity in the \( \gamma H2AX \) (Fig. 8A), it was hypothesized that they contain important contributors to the genotoxic effects of the pooled fractions. For this reason, SF18, SF19, SF22 and the respective mixtures were selected for further testing in the comet assay. As positive controls served UV-B irradiation for 1 min and exposure of the cells to 50 µM of H<sub>2</sub>O<sub>2</sub> for 1 h. The chemical positive control was applied to verify the FPG treatment. This was of importance because UV-B treatment did not induce FPG-sensitive sites in HepG2 cells like it does for example in HT-29 cells (Schwarz et al., 2012b). The effects caused by SM18 and SM19 followed a similar pattern as the corresponding fractions, and the two respective fractions and mixtures treated with FPG were not found to be significantly different from each other. Conclusively, in this case the overall effects can be attributed to the simultaneous presence of the seven different Alternaria mycotoxins added to the mixtures, resulting in combinatory effects. The significant increase in the tail intensity observed with FPG treatment could either be due to

oxidative damage or DNA adduct formation (e.g., N7-guanine adduct), which may subsequently lead to ring-open formamidopyrimidine structures (Collins, 2004; Louro et al., 2024). Of note, both perylene quinones, ATX-II and STTX-III, carry an epoxide group, which is postulated to form DNA-adducts and thereby impair DNA integrity. In fact, ATX-II was recently shown to form three covalent DNA adducts under cell-free conditions. Specifically, two adducts result though the binding of the epoxide group to guanin and one to cytosine (Soukup et al., 2020). Since rather high concentrations of ATX-II ( $\sim\!4.1~\mu M$  in F18/M19 and  $\sim\!6.7~\mu M$ in SF19/SM19) are present in the fractions/mixtures under closer investigation, the formation of DNA adducts seems plausible. As for SM22, no increase in tail intensity without FPG and only mild genotoxicity with FPG treatment was observed, and therefore, the outcome differed greatly from the effects of SF22 as well as from what was observed in the  $\gamma$ H2AX assay. The induction of  $\gamma$ H2AX caused by SM22 was negligible and lower than that caused by the original fraction SF22 (Fig. 8B). The greater differences between SF22 and SM22 in the comet assay may be explained by the fact that this assay can detect more types of DNA damage, and not only double-strand breaks as in the γH2AX assay (Collins, 2004). Since the mixtures consist of only seven selected Alternaria mycotoxins, it is likely that the most important mycotoxins responsible for the genotoxicity of SF22 were not included in the testing. Two suspected compounds are STTX-III, which is known to be present in the CE in relatively high concentrations, and ATX-III. The latter was previously found in an Alternaria alternata mycotoxin extract produced by the same strain used for the CE (Aichinger et al., 2019; Puntscher et al., 2019b; Schwarz et al., 2012b). However, due to a lack of availability, ATX-III was not included in the mycotoxin quantification of the CE and the fractions.

Of note, the fractions that induced genotoxicity (F8-10) were also found to suppress LPS-induced activation of the NF-kB signaling pathway (Fig. 3A). Inflammation is controlled and coordinated at multiple levels through multiple and intersecting pathways. In this context, the nuclear factor erythroid 2-related factor 2 (Nrf2) plays an important role in the defense machinery against oxidative stress, and the activation of the pathway was reported to suppress NF-κB signaling (Wardyn et al., 2015). Recently, the mycotoxin AOH was reported to induce the formation of reactive ROS in different cells lines and decrease the level of antioxidant glutathione (GSH), a potent defense mechanism against ROS. Furthermore, AOH and ATX-II are known to increase nuclear Nrf2 translocation and induce Nrf2 regulated genes (Groestlinger et al., 2022; Jarolim et al., 2017; Pahlke et al., 2016; Schwarz et al., 2012a; Tiessen et al., 2013) Thus, it is tempting to speculate that the immunosuppressive effects of both mycotoxins are interlinked with the activation of the Nrf2 pathway (Groestlinger et al., 2022).

#### 5. Conclusion

In conclusion, this study aimed to identify the critical mycotoxins or mixtures thereof responsible for the immunomodulatory, antiestrogenic and genotoxic effects induced by a naturally occurring complex extract (CE) of Alternaria mycotoxins. This is a crucial step toward the comprehension of the toxicological potential of the broad spectrum of molecules produced by these mold species. Based on the LC-MS/MS analysis of the known mycotoxins in the CE-fractions, obtained by RP-HPLC, and the results of previous studies, it could be excluded that the observed effects could be explained by the action of single substances. A comparison of the toxicological effects of the most active fractions and their corresponding mycotoxin mixtures revealed that, in some cases, combinations of several mycotoxins mimicking the different effects were identified. Specifically, mixtures of the seven Alternaria mycotoxins AOH, AME, TeA, AST, ATX-I, ATX-II and ALTP were elucidated as likely to be accountable. Conclusively, combinatory effects of several bioactive molecules seem to potentiate the effects caused by single substances emphasizing the importance of including mixture toxicology in the investigation of Alternaria mycotoxins. Of note, AST

was identified for the first time as an immunosuppressive and antiestrogenic Alternaria mycotoxin, possibly contributing to the effects caused by complex Alternaria toxin mixtures. Nevertheless, not all toxic effects could be related to known Alternaria toxins or mixtures thereof. Thus, it is likely that unidentified compounds or additional known mycotoxins, currently not available for testing, also played a role in these effects. Therefore, further studies are essential to gain a more comprehensive understanding of the chemical composition of natural Alternaria toxin mixtures and the individual and combinatory effects of its constituents. The results obtained in the present study provide useful data for assessing the risk associated with exposure to this class of mycotoxins, while also highlighting the need for further research into both the well-known and less studied compounds produced by this genus of molds. Future in vivo studies, along with a deeper understanding of the underlying molecular mechanisms, will be essential to confirm the current in vitro findings and provide a more comprehensive understanding of the potential health risks posed by these mycotoxins.

#### CRediT authorship contribution statement

Vanessa Partsch: Writing – original draft, Methodology, Investigation, Formal analysis, Data curation. Francesco Crudo: Writing – review & editing, Supervision, Methodology, Conceptualization. Daniel Piller: Investigation. Elisabeth Varga: Writing – review & editing, Methodology. Giorgia Del Favero: Writing – review & editing, Methodology. Doris Marko: Writing – review & editing, Supervision, Funding acquisition, Conceptualization.

#### Declaration of competing interest

The authors declare that they have no known competing financial interests or personal relationships that could have appeared to influence the work reported in this paper.

#### Acknowledgements

The authors thank the Mass Spectrometry Centre (MSC) and the Core Facility Multimodal Imaging, members of the VLSI (Vienna Life Science Instruments), Faculty of Chemistry, University of Vienna, for technical assistance during LC-MS/MS measurements and microscopy-based workflows. This research was supported by the University of Vienna.

#### Appendix A. Supplementary data

Supplementary data to this article can be found online at https://doi.org/10.1016/j.fct.2025.115315.

# Data availability

Data will be made available on request.

#### References

- Aichinger, G., Beisl, J., Marko, D., 2017. Genistein and delphinidin antagonize the genotoxic effects of the mycotoxin alternariol in human colon carcinoma cells. Mol. Nutr. Food Res. 61, 1600462. https://doi.org/10.1002/mnfr.201600462.
- Aichinger, G., Del Favero, G., Warth, B., Marko, D., 2021. Alternaria toxins-Still emerging? Compr. Rev. Food Sci. Food Saf. 20, 4390–4406. https://doi.org/ 10.1111/1541-4337.12803.
- Aichinger, G., Krüger, F., Puntscher, H., Preindl, K., Warth, B., Marko, D., 2019. Naturally occurring mixtures of *Alternaria* toxins: anti-estrogenic and genotoxic effects in vitro. Arch. Toxicol. 93, 3021–3031. https://doi.org/10.1007/s00204-019-02545-z.
- Altemöller, M., Podlech, J., Fenske, D., 2006. Total synthesis of altenuene and isoaltenuene. Eur. J. Org Chem. 1678–1684. https://doi.org/10.1002/ eioc.200500904.
- Arcella, D., Eskola, M., Gómez Ruiz, J.A., 2016. Dietary exposure assessment to Alternaria toxins in the European population. EFSA 14. https://doi.org/10.2903/j.efsa.2016.4654.

- Bai, X., Feldman, N.E., Chmura, K., Ovrutsky, A.R., Su, W.-L., Griffin, L., Pyeon, D., McGibney, M.T., Strand, M.J., Numata, M., Murakami, S., Gaido, L., Honda, J.R., Kinney, W.H., Oberley-Deegan, R.E., Voelker, D.R., Ordway, D.J., Chan, E.D., 2013. Inhibition of nuclear factor-kappa B activation decreases survival of Mycobacterium tuberculosis in human macrophages. PLoS One 8, e61925. https://doi.org/10.1371/journal.pone.0061925.
- Collins, A.R., 2004. The comet assay for DNA damage and repair: principles, applications, and limitations. Mol. Biotechnol. 26, 249–261. https://doi.org/10.1385/MB;26;3:249.
- Crudo, F., Dellafiora, L., Hong, C., Burger, L., Jobst, M., Del Favero, G., Marko, D., 2024. Combined *in vitro* and *in silico* mechanistic approach to explore the potential of *Alternaria* mycotoxins alternariol and altertoxin II to hamper γH2AX formation in DNA damage signaling pathways. Toxicol. Lett. 394, 1–10. https://doi.org/10.1016/j.toxlet.2024.02.008.
- Crudo, F., Partsch, V., Braga, D., Blažević, R., Rollinger, J.M., Varga, E., Marko, D., 2025. Discovery of the *Alternaria* mycotoxins alterperylenol and altertoxin I as novel immunosuppressive and antiestrogenic compounds in vitro. Arch. Toxicol. 99, 407–421. https://doi.org/10.1007/s00204-024-03877-1.
- Crudo, F., Varga, E., Aichinger, G., Galaverna, G., Marko, D., Dall'Asta, C., Dellafiora, L., 2019. Co-occurrence and combinatory effects of *Alternaria* mycotoxins and other xenobiotics of food Origin: current scenario and future perspectives. Toxins 604, 640. https://doi.org/10.3390/toxins11110640.
- Del Favero, G., Hohenbichler, J., Mayer, R.M., Rychlik, M., Marko, D., 2020. Mycotoxin altertoxin II induces lipid peroxidation connecting mitochondrial stress response to NF-κB inhibition in THP-1 macrophages. Chem. Res. Toxicol. 33, 492–504. https://doi.org/10.1021/acs.chemrestox.9b00378.
- Ebmeyer, J., Braeuning, A., Glatt, H., These, A., Hessel-Pras, S., Lampen, A., 2019. Human CYP3A4-mediated toxification of the pyrrolizidine alkaloid lasiocarpine. Food Chem. Toxicol. 130, 79–88. https://doi.org/10.1016/j.fct.2019.05.019.
- EFSA, 2011. Scientific Opinion on the risks for animal and public health related to the presence of Alternaria toxins in feed and food. EFSA J. 9. https://doi.org/10.2903/j. efsa.2011.2407.
- European Commission, 2023. Commission Regulation (EU) 2023/915 of 25 April 2023 on Maximum Levels for Certain Contaminants in Food and Repealing Regulation (EC) No 1881/2006: Commission Regulation (EU) 2023/915.
- Fehr, M., Pahlke, G., Fritz, J., Christensen, M.O., Boege, F., Altemöller, M., Podlech, J., Marko, D., 2009. Alternariol acts as a topoisomerase poison, preferentially affecting the IIalpha isoform. Mol. Nutr. Food Res. 53, 441–451. https://doi.org/10.1002/ mnfr.200700379.
- Fleck, S.C., Burkhardt, B., Pfeiffer, E., Metzler, M., 2012. Alternaria toxins: altertoxin II is a much stronger mutagen and DNA strand breaking mycotoxin than alternariol and its methyl ether in cultured mammalian cells. Toxicol. Lett. 214, 27–32. https://doi. org/10.1016/j.toxlet.2012.08.003.
- Groestlinger, J., Spindler, V., Pahlke, G., Rychlik, M., Del Favero, G., Marko, D., 2022. *Alternaria alternata* mycotoxins activate the aryl hydrocarbon receptor and nrf2-ARE pathway to alter the structure and immune response of colon epithelial cells. Chem. Res. Toxicol. 35, 731–749. https://doi.org/10.1021/acs.chemrestox.1c00364.
- Gruber-Dorninger, C., Novak, B., Nagl, V., Berthiller, F., 2017. Emerging mycotoxins: beyond traditionally determined food contaminants. J. Agric. Food Chem. 65, 7052–7070. https://doi.org/10.1021/acs.jafc.6b03413.
- Hellwig, V., Grothe, T., Mayer-Bartschmid, A., Endermann, R., Geschke, F.-U., Henkel, T., Stadler, M., 2002. Altersetin, a new antibiotic from cultures of endophytic *Alternaria spp.* Taxonomy, fermentation, isolation, structure elucidation and biological activities. J. Antibiot. 55, 881–892. https://doi.org/10.7164/ antibiotics.55.881.
- Hernandez-Ramirez, G., Pazos-Castro, D., Gonzalez-Klein, Z., Resuela-Gonzalez, J.L., Fernandez-Bravo, S., Palacio-Garcia, L., Esteban, V., Garrido-Arandia, M., Tome-Amat, J., Diaz-Perales, A., 2022. Alt a 1 promotes allergic asthma *in vivo* through TLR4-alveolar macrophages. Front. Immunol. 13, 877383. https://doi.org/10.3389/ fimmu.2022.877383.
- Hessel-Pras, S., Kieshauer, J., Roenn, G., Luckert, C., Braeuning, A., Lampen, A., 2019. In vitro characterization of hepatic toxicity of Alternaria toxins. Mycotoxin Res. 35, 157–168. https://doi.org/10.1007/s12550-018-0339-9.
- Hohenbichler, J., Aichinger, G., Rychlik, M., Del Favero, G., Marko, D., 2020. Alternaria alternata toxins synergistically activate the aryl hydrocarbon receptor pathway in vitro. Biomolecules 10, 1018. https://doi.org/10.3390/biom10071018.
- Hong, Y., Han, H.-J., Lee, H., Lee, D., Ko, J., Hong, Z.-Y., Lee, J.-Y., Seok, J.-H., Lim, H.S., Son, W.-C., Sohn, I., 2020. Deep learning method for comet segmentation and comet assay image analysis. Sci. Rep. 10, 18915. https://doi.org/10.1038/s41598-020-75592-7.
- Hu, W., Sorrentino, C., Denison, M.S., Kolaja, K., Fielden, M.R., 2007. Induction of cyp1a1 is a nonspecific biomarker of aryl hydrocarbon receptor activation: results of large scale screening of pharmaceuticals and toxicants in vivo and in vitro. Mol. Pharmacol. 71, 1475–1486. https://doi.org/10.1124/mol.106.032748.
- Jarolim, K., Del Favero, G., Pahlke, G., Dostal, V., Zimmermann, K., Heiss, E., Ellmer, D., Stark, T.D., Hofmann, T., Marko, D., 2017. Activation of the Nrf2-ARE pathway by the Alternaria alternata mycotoxins altertoxin I and II. Arch. Toxicol. 91, 203–216. https://doi.org/10.1007/s00204-016-1726-7.
- Kollarova, J., Cenk, E., Schmutz, C., Marko, D., 2018. The mycotoxin alternariol suppresses lipopolysaccharide-induced inflammation in THP-1 derived macrophages targeting the NF-κB signalling pathway. Arch. Toxicol. 92, 3347–3358. https://doi. org/10.1007/s00204-018-2299-4.
- Lee, S.-Y., Cherla, R.P., Tesh, V.L., 2007. Simultaneous induction of apoptotic and survival signaling pathways in macrophage-like THP-1 cells by Shiga toxin 1. Infect. Immun. 75, 1291–1302. https://doi.org/10.1128/iai.01700-06.

- Lehmann, L., Wagner, J., Metzler, M., 2006. Estrogenic and clastogenic potential of the mycotoxin alternariol in cultured mammalian cells. Food Chem. Toxicol. 44, 398–408. https://doi.org/10.1016/j.fct.2005.08.013.
- Liu, Y., Rychlik, M., 2015. Biosynthesis of seven carbon-13 labeled Alternaria toxins including altertoxins, alternariol, and alternariol methyl ether, and their application to a multiple stable isotope dilution assay. Anal. Bioanal. Chem. 407, 1357–1369. https://doi.org/10.1007/s00216-014-8307-5.
- Louro, H., Vettorazzi, A., López de Cerain, A., Spyropoulou, A., Solhaug, A., Straumfors, A., Behr, A.-C., Mertens, B., Žegura, B., Fæste, C.K., Ndiaye, D., Spilioti, E., Varga, E., Dubreil, E., Borsos, E., Crudo, F., Eriksen, G.S., Snapkow, I., Henri, J., Sanders, J., Machera, K., Gaté, L., Le Hegarat, L., Novak, M., Smith, N.M., Krapf, S., Hager, S., Fessard, V., Kohl, Y., Silva, M.J., Dirven, H., Dietrich, J., Marko, D., 2024. Hazard characterization of Alternaria toxins to identify data gaps and improve risk assessment for human health. Arch. Toxicol. 98, 425–469. https://doi.org/10.1007/s00204-023-03636-8.
- Marfori, E.C., Kajiyama, S., Fukusaki, E., Kobayashi, A., 2002. Trichosetin, a novel tetramic acid antibiotic produced in dual culture of *Trichoderma harzianum* and *Catharanthus roseus* Callus. Zeitschrift fur Naturforschung. C. J. Biosci. 57, 465–470. https://doi.org/10.1515/xpc-2002-5-611.
- Nemecek, G., Thomas, R., Goesmann, H., Feldmann, C., Podlech, J., 2013. Structure elucidation and total synthesis of altenuic acid III and studies towards the total synthesis of altenuic acid II. Eur. J. Org Chem. 6420–6432. https://doi.org/10.1002/ejoc.201300879, 2013.
- Ostry, V., 2008. Alternaria mycotoxins: an overview of chemical characterization, producers, toxicity, analysis and occurrence in foodstuffs. World Mycotoxin J. 1, 175–188. https://doi.org/10.3920/WMJ2008.x013.
- Pahlke, G., Tiessen, C., Domnanich, K., Kahle, N., Groh, I.A.M., Schreck, I., Weiss, C., Marko, D., 2016. Impact of *Alternaria* toxins on CYP1A1 expression in different human tumor cells and relevance for genotoxicity. Toxicol. Lett. 240, 93–104. https://doi.org/10.1016/j.toxlet.2015.10.003.
- Park, S.-W., Kim, Y.I., 2013. Triptolide induces apoptosis of PMA-treated THP-1 cells through activation of caspases, inhibition of NF-κB and activation of MAPKs. Int. J. Oncol. 43, 1169–1175. https://doi.org/10.3892/ijo.2013.2033.
- Pfeiffer, E., Eschbach, S., Metzler, M., 2007. Alternaria toxins: DNA strand-breaking activity in mammalian cells in vitro. Mycotoxin Res. 23, 152–157. https://doi.org/ 10.1007/BF02951512.
- Puntscher, H., Aichinger, G., Grabher, S., Attakpah, E., Krüger, F., Tillmann, K., Motschnig, T., Hohenbichler, J., Braun, D., Plasenzotti, R., Pahlke, G., Höger, H., Marko, D., Warth, B., 2019a. Bioavailability, metabolism, and excretion of a complex *Alternaria* culture extract versus altertoxin II: a comparative study in rats. Arch. Toxicol. 93, 3153–3167. https://doi.org/10.1007/s00204-019-02575-7.
- Puntscher, H., Hankele, S., Tillmann, K., Attakpah, E., Braun, D., Kütt, M.-L., Del Favero, G., Aichinger, G., Pahlke, G., Höger, H., Marko, D., Warth, B., 2019b. First insights into *Alternaria* multi-toxin *in vivo* metabolism. Toxicol. Lett. 301, 168–178. https://doi.org/10.1016/j.toxlet.2018.10.006.
- Puntscher, H., Kütt, M.-L., Skrinjar, P., Mikula, H., Podlech, J., Fröhlich, J., Marko, D., Warth, B., 2018. Tracking emerging mycotoxins in food: development of an LC-MS/MS method for free and modified *Alternaria* toxins. Anal. Bioanal. Chem. 410, 4481–4494. https://doi.org/10.1007/s00216-018-1105-8.
- Qin, Y., Zhou, Z.-W., Pan, S.-T., He, Z.-X., Zhang, X., Qiu, J.-X., Duan, W., Yang, T., Zhou, S.-F., 2015. Graphene quantum dots induce apoptosis, autophagy, and inflammatory response via p38 mitogen-activated protein kinase and nuclear factor-

- $\kappa B$  mediated signaling pathways in activated THP-1 macrophages. Toxicology 327, 62–76. https://doi.org/10.1016/j.tox.2014.10.011.
- Schreck, I., Deigendesch, U., Burkhardt, B., Marko, D., Weiss, C., 2012. The Alternaria mycotoxins alternariol and alternariol methyl ether induce cytochrome P450 1A1 and apoptosis in murine hepatoma cells dependent on the aryl hydrocarbon receptor. Arch. Toxicol. 86, 625–632. https://doi.org/10.1007/s00204-011-0781-3.
- Schwarz, C., Kreutzer, M., Marko, D., 2012a. Minor contribution of alternariol, alternariol monomethyl ether and tenuazonic acid to the genotoxic properties of extracts from *Alternaria alternata* infested rice. Toxicol. Lett. 214, 46–52. https://doi. org/10.1016/j.jtoxlet.2012.08.002.
- Schwarz, C., Tiessen, C., Kreutzer, M., Stark, T., Hofmann, T., Marko, D., 2012b. Characterization of a genotoxic impact compound in *Alternaria alternata* infested rice as Altertoxin II. Arch. Toxicol. 86, 1911–1925. https://doi.org/10.1007/s00204-012.0958.4
- Solhaug, A., Vines, L.L., Ivanova, L., Spilsberg, B., Holme, J.A., Pestka, J., Collins, A., Eriksen, G.S., 2012. Mechanisms involved in alternariol-induced cell cycle arrest. Mutation Res. 738–739, 1–11. https://doi.org/10.1016/j.mrfmmm.2012.09.001.
- Soukup, S.T., Fleck, S.C., Pfeiffer, E., Podlech, J., Kulling, S.E., Metzler, M., 2020. DNA reactivity of altertoxin II: identification of two covalent guanine adducts formed under cell-free conditions. Toxicol. Lett. 331, 75–81. https://doi.org/10.1016/j.toxlet.2020.05.018
- Suchar, L.A., Chang, R.L., Thomas, P.E., Rosen, R.T., Lech, J., Conney, A.H., 1996. Effects of phenobarbital, dexamethasone, and 3-methylcholanthrene administration on the metabolism of 17 beta-estradiol by liver microsomes from female rats. Endocrinology 137, 663–676. https://doi.org/10.1210/endo.137.2.8593816.
- Tice, R.R., Agurell, E., Anderson, D., Burlinson, B., Hartmann, A., Kobayashi, H., Miyamae, Y., Rojas, E., Ryu, J.-C., Sasaki, Y.F., 2000. Single cell gel/comet assay: guidelines for in vitro and in vivo genetic toxicology testing. Environ. Mol. Mutagen. 35, 206–221. https://doi.org/10.1002/(SICI)1098-2280(2000)35:3<206:AID-EM8>3.0.CO;2-J.
- Tiessen, C., Fehr, M., Schwarz, C., Baechler, S., Domnanich, K., Böttler, U., Pahlke, G., Marko, D., 2013. Modulation of the cellular redox status by the *Alternaria* toxins alternariol and alternariol monomethyl ether. Toxicol. Lett. 216, 23–30. https://doi.org/10.1016/j.toxlet.2012.11.005.
- Tsuchiya, Y., Nakajima, M., Yokoi, T., 2005. Cytochrome P450-mediated metabolism of estrogens and its regulation in human. Cancer Lett. 227, 115–124. https://doi.org/10.1016/j.canlet.2004.10.007.
- Vesonder, R.F., Tjarks, L.W., Rohwedder, W.K., Burmeister, H.R., Laugal, J.A., 1979. Equisetin, an antibiotic from *Fusarium equiseti* NRRL 5537, identified as a derivative of N-methyl-2,4-pyrollidone. J. Antibiot. 32, 759–761. https://doi.org/10.7164/ontibiotics 23.759.
- Wardyn, J.D., Ponsford, A.H., Sanderson, C.M., 2015. Dissecting molecular cross-talk between Nrf2 and NF-kB response pathways. Biochem. Soc. Trans. 43, 621–626. https://doi.org/10.1042/BST20150014.
- Wormke, M., Castro-Rivera, E., Chen, I., Safe, S., 2000. Estrogen and aryl hydrocarbon receptor expression and crosstalk in human Ishikawa endometrial cancer cells.

  J. Steroid Biochem. Mol. Biol. 72, 197–207. https://doi.org/10.1016/S0960-0760
- Wormke, M., Stoner, M., Saville, B., Walker, K., Abdelrahim, M., Burghardt, R., Safe, S., 2003. The aryl hydrocarbon receptor mediates degradation of estrogen receptor alpha through activation of proteasomes. Mol. Cell Biol. 23, 1843–1855. https://doi.org/10.1128/MCB.23.6.1843-1855.2003.